Sorbents for CO2 capture from flue gas – Aspects from materials and theoretical chemistry

Article *in* Nanoscale · October 2010

DOI: 10.1039/c0nr00042f · Source: PubMed

Sorbents for CO_2 capture from flue gas—aspects from materials and theoretical chemistry

Niklas Hedin,* LiJun Chen and Aatto Laaksonen

Received 20th January 2010, Accepted 31st March 2010
DOI: 10.1039/c0nr00042f

Predictions of future climate change have triggered a search for ways to reduce the release of greenhouse gases into the atmosphere. Carbon capture and storage (CCS) assists this goal by reducing carbon dioxide emissions, and CO_2 adsorbents in particular can reduce the costs of CO_2 capture. Here, we review the nanoscale sorbent materials that have been developed and the theoretical basis for their function in CO_2 separation, particularly from N_2-rich flue gases.

1. Introduction

Cost-effective large-scale separation and capture of CO_2 from gas mixtures, followed by storage (and possibly recycling of the carbon and the oxygen) are of the utmost importance, due to the increasing impact of CO_2, a greenhouse gas, on global warming.[1,2] It is a priority to find inexpensive, effective, and robust materials and technologies that reduce emissions of CO_2 and other greenhouse gases and that are suitable for installation in power plants and industries that rely on fossil fuels.[3,4]

Three types of gas mixtures are targets for capture and separation technologies: the components of flue gases (mainly CO_2/N_2) and natural gases (mainly CH_4/CO_2), and precombustion gas mixtures that contain H_2. The aim for precombustion separation is to develop materials that adsorb and separate H_2, which is important for certain new CCS precombustion capture procedures. Aside from the components in flue gases, natural gases, and hydrogen, many other gases can be found in gas mixtures. For example, water is found in small amounts in most systems. Water generally leads to complications in separation applications, although under certain circumstances it may contribute constructively to the process. Surprisingly, only a few computational investigations have included water in detailed studies of its role in this regard.

The use of appropriate nanostructured materials may potentially reduce the costs associated with CCS. For example, membranes or adsorption-driven processes may be used to separate CO_2 from N_2-rich flue gases.[5] CO_2 is currently separated from N_2-rich gases *via* absorption by aqueous solutions of, for example, simple alkanolamines or chilled NH_3.[2] If increased CO_2 selectivity can be achieved, adsorption-mediated separation of CO_2 from flue gases can potentially separate CO_2 from N_2 at a much lower cost than that associated with current technologies.[6] Recent efforts to develop adsorbent materials have focused on zeolites, metal organic frameworks (MOFs), and hybrid systems, as well as highly alkaline adsorbents. Alkaline hybrid systems may selectively adsorb CO_2 over N_2. Carbon and silica materials are also of great interest in this regard. Among solution-based

Department of Materials and Environmental Chemistry, Berzelii Center EXSELENT on Porous Materials, Arrhenius Laboratory, Stockholm University, S-106 91 Stockholm. E-mail: niklas.hedin@mmk.su.se

Niklas Hedin

Niklas Hedin, MSc. Chemical Engineering and PhD Physical Chemistry from the Royal Institute of Technology, Stockholm, Sweden. Post doctoral research with Bradley Chmelka in University of California at Santa Barbara, US (2001–2003) and with Sebastian Reyes at ExxonMobil Corporate Research Laboratories in Annadale, US (2004–2006). Now Associate Professor in Materials Chemistry, Department of Materials and Environmental Chemistry at Stockholm University, Sweden. Main research interest is adsorbents that could allow a cost effective separation of CO_2 from N_2-rich gases; special focus on molecular details on solid–gas interactions.

LiJun Chen

LiJun Chen was born in Zhejiang, China in 1979. She obtained a Bachelor's degree in Applied Chemistry in 2002 and PhD in Physical Chemistry in 2007 at Jilin University. Since 2007 she has been working as a postdoctoral student in the Department of Materials and Environment Chemistry, Stockholm University. Her main research interests covered the development of multi-scale simulation methods bridging molecular dynamics, dissipative particle dynamics with the application in simulations of macromolecules. Now she focuses on the theoretical studies of the porous materials combining quantum chemistry, molecular dynamics and Monte Carlo approaches.

technologies, ionic liquids may potentially be used for CO_2 capture. Here, we review the adsorbents for CCS that have been described in the literature, with an emphasis on both materials and computational investigations into the uptake and selectivity of CO_2 from N_2-rich gases.

The free energy of gas molecules decreases in the presence of the attractive electronic environment at an interface.[7] The density of gas molecules increases close to an interface, and the average diffusion length of each molecule decreases. Development of a surface excess is called "adsorption" and is an exothermic process that arises as a consequence of attractive interactions and the associated loss of entropy.[7] Adsorption is typically divided into physi- and chemisorption, in which no chemical bonds are formed during physisorption. During chemisorption, the gas and the adsorbents undergo electronic reconfiguration. Both types of adsorption are relevant to CO_2 separation. Adsorbents contain nanoscale morphological features and are typically divided into three classes based on pore size: according to the International Union of Pure and Applied Chemistry (IUPAC), microporous materials have pores smaller than 2 nm, mesoporous materials have pores between 2 and 50 nm, and macroporous materials have pores larger than 50 nm. For CO_2 capture, sorbents with high specific surface areas have proven to be the most promising.[8–14]

The main workhorses in computational studies of carbon capture and separation are molecular dynamics (MD) simulations, grand canonical Monte Carlo (GCMC) simulations,[15,16] and *ab initio* quantum chemistry (QC) calculations at suitable levels of theory. In QC, density functional theory (DFT) is the first choice because it includes electron correlation effects. However, DFT demands care when applied to systems that contain hydrogen bonds or weak interactions. All modeling methods (MC, MD, and QC) can be used either independently or in conjunction with experiments (in complementarity) to gain information at the molecular level. The large data sets obtained from these traditional calculations may be used in newer methods, such as kinetic Monte Carlo (kMC) simulations. The kMC method requires a detailed knowledge of the system, including all stationary states on the free energy surface and the barriers that separate these states.

Transition state theory (TST) can be applied in kMC simulations, and has been used in adsorption studies reported in the literature.[17] MC simulations performed in the grand canonical ensemble yield statistical and ensemble properties of the adsorption and desorption processes and predict the preferred locations of adsorption. MD simulations model the transport properties (such as diffusion) of gases as they interact with (are captured by) a sorbent material. Selective capture requires that target captured gases quickly find their way (*i.e.*, are "channeled") to the area of a surface designed for absorption. Optimally, other gas components encounter this surface more slowly or at a later time.

MD simulations are useful at several stages of the modeling process. After constructing the molecular structure and framework of an adsorbent substrate, it is important to submit the material to repeated simulated annealing steps to test the stability and robustness of the model substrate prior to introducing gas molecules. An accurate model for the adsorbate is also very important. For example, CO_2 does not have an electric dipole moment; however, it has a large electric quadrupole moment that arises from the strong dipole moments of the C=O bonds. At short distances, O=C=O is locally highly polar and requires an accurate description of the electrostatic component of its force field (FF) used in a simulation. This is especially important when CO_2 is present in zeolites, which have a strong ionic character due to the zeolite metal atoms or additional ions hosted in the structure.

A major component of many gas mixtures is N_2. Although it appears to be a simple molecule, the triple bond sometimes complicates the theoretical calculation of its molecular properties. N_2 often serves as a benchmark molecule for new computational schemes. *Ab initio* calculations and simulations can be applied when additional levels of detail are required for modeling the structures or interactions in a simulation. QC calculations are important for distinguishing chemisorption from physisorption, because these calculations permit evaluation of the electronic rearrangements associated with a particular process. Most importantly, QC calculations aid investigations into reaction mechanisms; *e.g.*, the mechanisms that underlie catalyzed reactions. QC calculations are routinely used to develop FFs for atomic charges or to fine-tune descriptions of bonded interactions. Empirical FFs are the most important component of a computer simulation, because the integrity of the simulation results depends directly and critically on these FFs.

During the past decade, significant progress has been made in the development of FFs that describe the adsorption of greenhouse gases. Several improved parameterizations have been suggested for zeolites, MOFs, and silicas, which will be discussed in this review. As an example of the parameterization, García-Sánchez *et al.*[18] recently developed a complete FF that accurately reproduced the adsorption properties of CO_2 in a variety of zeolites with various topologies and compositions. The FF parameters were obtained by numerical optimization using their own experimental data, and were subsequently validated by comparison with available literature data. Their model explicitly distinguished silicon from aluminium using different charge for

Aatto Laaksonen

Aatto Laaksonen is a Professor in Physical Chemistry at Stockholm University; BSc. Mathematics, Stockholm University; PhD in Physical Chemistry Stockholm University 1981; postdoctoral research with Dr Victor Saunders 1982, Daresbury Laboratory, UK; postdoctoral research with Dr Enrico Clementi 1983–1985, IBM research laboratories in Poughkeepsie and in Kingston, USA. Active in the area of computational materials science, being responsible for modelling work to design new nano- and mesoporous materials for separation and storage of gases and for heterogeneous catalysis processes inside the pores within the newly established center-of-excellence at Stockholm University.

oxygen atoms bridging two silicon atoms (q_{OSi}) and oxygen atoms bridging one silicon and one aluminium atom (q_{OAl}). The Lennard-Jones interactions between CO_2 and the zeolite were modeled by only taking into account the interactions between carbon dioxide and O atoms and Na cations of the zeolite. An essential feature of their model was the mobility of the Na cations in the framework, which they claimed to be vital to reproduce accurately adsorption of carbon dioxide in faujasites. The FF was fully transferable between zeolite framework types and was applicable to all possible Si/Al ratios (with sodium as an extra-framework cation).

This review focuses mainly on the work performed in the first decade of this century. During this period, many novel types of nanoscale materials have been discovered and tested for potential application to separation and temporary storage technologies. We review the material development, modeling, and simulation efforts. The extensive range of related engineering literature is not reviewed here; for this, we refer the reader to other reviews.[2,19,20,21]

2. Sorbents for CO_2 capture from flue gases

A variety of sorbents have been investigated as potential CO_2 capture substrates for use with flue gases in pressure swing or temperature swing adsorption processes.[4,7,22] Successful adsorbents must fulfil a range of chemical, chemical engineering, and solid mechanics criteria. As an introduction, we refer the reader to an excellent but only partly overlapping review by Choi *et al.*, which considered adsorbents for the adsorptive capture of CO_2 from large point sources.[23] We review the theoretical advances in combination with aspects from material chemistry.

Adsorbents can be categorized in many ways, including by composition (as in the present study) or by pore dimensions. Zeolites, carbon molecular sieves (CMSs), and MOFs are examples of microporous adsorbents with molecule-sized pore windows. These materials have been shown to separate gas molecules by equilibrium, kinetic, or molecular sieving mechanisms. Gas molecules have different effective kinetic diameters, and CO_2 appears to have the smallest kinetic diameter. CO_2, N_2, and CH_4 have effective kinetic diameters in zeolites of 0.33, 0.365, and 0.38 nm, respectively.[24] The exact values are under discussion and appear to be substrate dependent.[4,24,25] For simulations of gas molecules in sorbents, several well-known sorbate models, and force fields, for the sorbate–sorbate and sorbate–sorbent interactions have been developed and used. Intermolecular interactions are usually represented by a Lennard-Jones term and an electrostatic term:

$$u_{ij}(r) = \sum_{i,j}\left\{4\varepsilon_{ij}\left(\frac{\sigma_{ij}}{r_{ij}}\right)^{12} - \left(\frac{\sigma_{ij}}{r_{ij}}\right)^{6} + \frac{q_i q_j}{4\pi\varepsilon_0 r_{ij}}\right\}$$

$\varepsilon_0 = 8.8542 \times 10^{-12}\ C^2\ N^{-1}\ m$ is the permittivity of vacuum. Table 1 lists the most used CO_2, N_2, CH_4 models in literature. CO_2 has a quadruple moment -1.43×10^{-39} C m^2, the quadruple moment of N_2 is -4.67×10^{-40} C m^2, CH_4 does not have a quadruple moment. The polarizabilities of CO_2, N_2, CH_4 are 29.11×10^{25} cm^{-3}, 17.403×10^{25} cm^{-3}, 25.93×10^{25} cm^{-3} respectively. Mesoporous materials have larger pores that allow rapid gas diffusion, with pores that are organized and oriented with the help of surfactants or amphiphilic polymers.[26,27] Table 2 lists the materials to be discussed in the present analysis.

In simulation of zeolites and carbons, the Lennard-Jones and partial charges of the individual atoms are either derived from *ab initio* calculations[28] or from "fitting" to experimental isotherms.[18,29] For MOF frameworks, the Lennard-Jones parameters are often extracted from generic force fields, in particular UFF[30] or DREIDING,[31] that contain parameters for the whole periodic table.[17,32,33,34] Salles *et al.*[35,36] made use of the intramolecular and nonbonded parameters, for a particular organic moiety, from the Consistent Valence Force Field (cvff).[37] The interactions between inorganic and organic ligands, including bond stretching, angle bending, a torsion term and nonbonded parameters, were adjusted from the DREIDING force field in order to reproduce the structural features of both large and narrow pore forms of MIL-53. The modeling captures accurately the swelling/shrinkage of the structure. The partial charges of the framework atoms were usually calculated from DFT using Hirshfeld,[38] Mulliken,[39] ChelpG[40] and Merz–Kollman[41] charge calculating methods.[17,34,42] In particular, an efficient and systematic first principles parameterization of force fields based on MM3[43] for MOFs using a genetic algorithm approach was proposed by Tafipolsky and Schmid[44]

The economical separation of CO_2 from point sources, using adsorbent-driven processes, imposes many demands on the sorbent. Both the uptake capacity for CO_2 and the preferential CO_2-over-N_2 selectivity are important for economical pressure

Table 1 Interaction potential parameters for CO_2, N_2 and CH_4

Adsorbate	Model	σ/nm	(ε/k_B)/K	q/e	Ref.
C–C (CO_2)	EPM2[47,a]	0.2785	28.999	+0.6645	17,18,35,36,29,28
O–O (CO_2)	EPM2[47]	0.3064	82.997	−0.33225	17,18,35,36,29,28
C–C (CO_2)	Maurin *et al.*[48,b]	0.383	46.601	+0.72	42,46,47
O–O (CO_2)	Maurin *et al.*[48]	0.336	76.452	−0.36	42,46,47
C–C (CO_2)	TraPPE[49,50,c]	0.280	27.0	+0.70	33,32,29,34
O–O (CO_2)	TraPPE[49,50]	0.305	79.0	−0.35	33,32,29,34
N–N (N_2)	Murthy *et al.*[51,d]	0.332	36.4	−0.482	29,28
CH_4–CH_4	TraPPE[49,50]	0.373	148.0	0	29
CH_4–CH_4	Jiang *et al.*[52]	0.3812	148.2	0	32

[a] The parameters were fitted to the experimental VLE data of bulk CO_2. [b] The parameters were fitted to reproduce the solid CO_2 structure. [c] The parameters were fitted to reproduce the vapor–liquid coexistence curves. [d] N_2 was represented as a three-site model, with a positive charge ($q^+ = 2q^-$) in the middle of the N–N bond.

Table 2 CO_2 sorbents[a]

Sorbent	T/K	p_{CO_2}/kPa	n/mmol g^{-1}	Ref.
Zeolites and all-silica microporous solids				
NaX	306; 295	67; 100	5.4; 4.5	8,9
NaY; HY	295; 295	100; 100	4.0; 1.1	9
Na-ZSM-5; H-ZSM-5	297; 295	0.67; 100	1.8;1.9	8,9
Silicalite	295	100	1.4	8,9
NaA	298	93	4.1	10
β-zeolite	303	100	1.8	53
Na-mordendite	308	1000	2.8	54
Herschelite	298	690	2.0	55
ITQ-6; ITQ-6/AP	293; 293	100; 100	1.1; 1.2	56
Aluminium phosphates				
$ALPO_4$-5	165 K, $P/P_0 = 0.06$		3.3	57
$ALPO_4$-14	290	100	2.2	58
$SAPO_4$-34	298	100	3.4	59
STA-7	303	2800	7.5	60
Metal–organic frameworks				
MOF-177	298	3000	32	11
IRMOF-1/MOF-5	298	3000	21	11
IRMOF-6	298	3000	18	11
IRMOF-3	298	3000	18	11
ZIF-69	273	100	3.1	61
ZIF-20	273	100	3.1	61
ZIF-100	298	110	0.95	62
MIL-53	304	1600	9.0	63
MIL-100	303	6000	18	12
MIL-101(Cr)	298	5000	40	12
$Cu_2(BTC)_2$	298	3000	11	11
Imidazolate MOF	253	100	4.9	64
Covalent organic frameworks and porous organics				
COF-10/102/103	298	5500	22–27	13
Carbons				
BF CMS	298	280	2.6	65
PX21	303	5000	15	14
BPL	303	5000	10	14
CFCMS	298	5700	11	66
AC3000 (carbon)	303	4000	11.7	67
Graphene	195	100	8.0	68
CMK-3	298	100	1.7	69
Amine modified mesoporous silica				
SBA-12/AP	298	N/A	max: 1.0	70
MCM-41/PEI	348	N/A	215 mg g^{-1}-PEI	71
SBA-15/Hyperbranched amines	298	N/A	3.1	72
MCM-48/AP	298	100	2.2	73
Xerogel/AP	298	100	1.2	73
AMS	298	N/A	1.25	74
MCM-41/pore expanded/TRI	358	N/A	2.7	75,76
MCM-41/pore expanded/DEA	298	100	3.25	77,78
Silica monolith/TEPA	348	N/A	260 mg g^{-1} sorbent	79
Other sorbents				
HTlc	673	100	1.5	80
CARiACT/PEI	313	N/A	3.1	81
Diaion/PEI	313	N/A	2.5	82
MCM-41 Silica	298	2500	9.6	83,84
Amine-modified hydrothermal carbon	253	100	4.1	85

[a] Note: AP = n-propyl amine; PEI = polyethyleneimine; for other abbreviations see the text or the references.

or temperature swing adsorption processes. Wiley *et al.* showed that increasing the CO_2 selectivity of the adsorbents could radically lower the costs of separation.[6] Sensitivity to water, cost, and recyclability are important economical factors. Although the engineering aspects of adsorbent-driven CO_2 separation are not considered here, this field of research would benefit substantially from closer collaboration between engineers and chemists.

2.1. Zeolites and all-silica microporous solids

Zeolites are microporous aluminosilicates that occur naturally, but can also be synthesized in the laboratory. Zeolites contain a network of interconnecting channels or cages that can be used to separate gas molecules *via* equilibrium, kinetic, or molecular sieving mechanisms. Zeolites are typically described by the

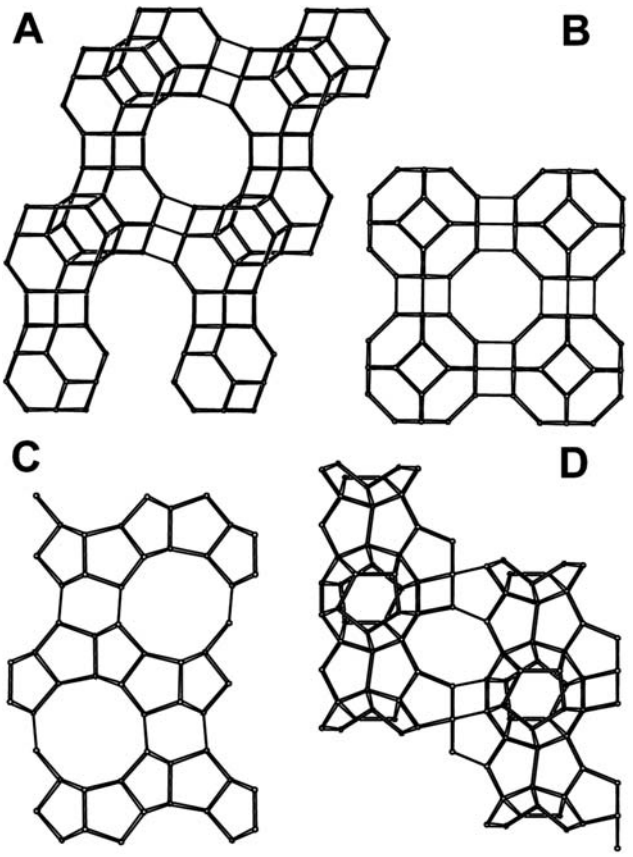

Fig. 1 Zeolite structures: (A) zeolite X, structural code FAU; (B) zeolite A, structural code LTA; (C) ZSM-5, structural code MFI; (D) ZSM-58, structural code DDR. Redrawn from the Database of Zeolite Structures[85] with permission.

number of oxygen atoms encircling the smallest windows that form a percolating network: 8-, 10-, and 12-ring zeolites. Zeolites are described as having either cages or channels. In zeolites of the cage type, the pore window is an aperture that constricts the diffusive paths. Channel-type zeolites contain a locally tubular diffusive path. Fig. 1 shows the structures of some of the zeolites discussed in this review.

Zeolite X (Fig. 1a) is the most widely studied sorbent for CO_2 capture. It has a caged structure (structural code FAU,[85] Faujasite) and window apertures defined by 12-membered rings, which allow unhindered access for CH_4, N_2, CO_2, and H_2O. Zeolite X has a Si/Al ratio of 1.3,[86] and the presence of alumina gives the framework a negative charge. The cations of zeolite X affect the heat of adsorption for CO_2, such that increases in the heat of adsorption result from increased monovalent charge densities.[8,87] Harlick and Tezel concluded that NaX or NaY were the best adsorbents for separation processes (Fig. 2).[9] Cavenati *et al.* showed that NaX yielded CO_2-over-N_2 adsorption selectivity at pressures as high as 3.2 MPa at 298 K.[88] The adsorption of CO_2 was shown to be higher in NaX than in NaZSM-5, even though the heats of adsorption were similar.[8] Brandani and Ruthven studied the uptake of CO_2 in NaX, CaX, LiLSX, and NaLSX (zeolite LSX had a Si/Al ratio of 1) and recognized that water compromised the uptake of CO_2.[89] When water was adsorbed, the electric field gradients decreased and CO_2, with its significant electric quadrupolar moment, was less prone to adsorb. The presence of water vapor in CO_2 capture processes could be a serious problem for NaX.

Papadopoulos and Theodorou[90] investigated the sorption dynamics of CH_4, CO_2, H_2, and D_2 in the frameworks of ITQ-1 and NaX zeolites using atomistic and mesoscopic computer simulations. They found that the loading dependence of self-diffusivity (D_s) was affected by the energetic inhomogeneity of the sorption sites and/or the site topology. The diffusion and adsorption of CO_2 inside the pores of Li^+, Na^+, and K^+ ion-exchanged X-type zeolites were simulated by Nakazaki and others[91] using MD and MC simulation methods. CO_2 was found to diffuse into the zeolite pores, collide with pore walls, and remain trapped in the supercages of the zeolite structures. CO_2 was found to adsorb strongly near the 3B site of the Li^+ ions. MD simulations by Jia and Murad[92] studied gas separation using zeolite membranes (FAU) and two binary mixtures: O_2/N_2 and CO_2/N_2. These mixtures were found to exhibit different behavior in the presence of the membrane. For the O_2/N_2 mixture, adsorption and loading in the membrane were similar for both O_2 and N_2. The observed drop in selectivity resulted from interactions between gas molecules: O_2 slowed the rate of diffusion of N_2, while N_2 slightly increased the rate of diffusion of O_2 when passing through the pores. CO_2, on the other hand, was selectively adsorbed and loaded in the zeolite, and did not leave much space for N_2 adsorption. While N_2 continued to have a higher diffusion rate than CO_2, so few N_2 molecules were present in the zeolite that the selectivity showed a significant increase. Similar to the above study, Jia and Murad[93] investigated gas separation efficiencies in three aluminium-rich zeolite membranes by MD simulation, with the aim of studying the effects of pore size, pore structure, state condition, and composition on the permeation of two binary gas mixtures: O_2/N_2 and CO_2/N_2. (The three membranes consisted of zeolites with different structures and structural codes: FAU, MFI, and CHA.)

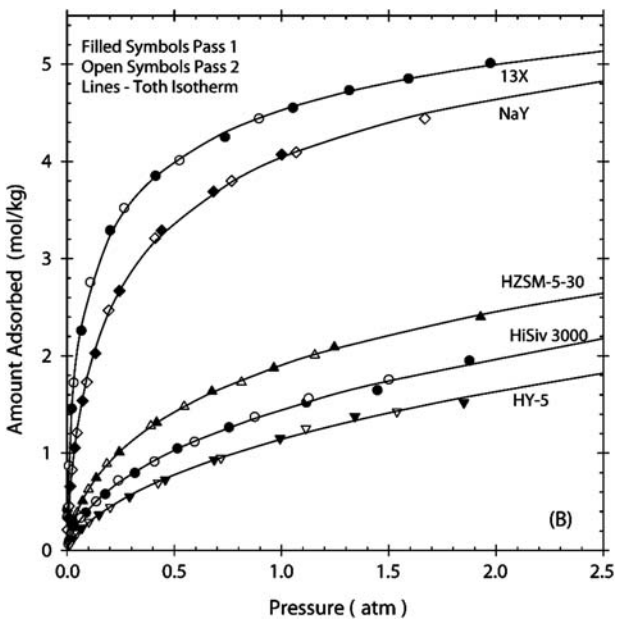

Fig. 2 Carbon dioxide adsorption isotherms for different zeolites. From Harlick and Tezel,[9] reprinted with permission.

Zeolite Y has the same general structure as zeolite X, but the Si/Al ratio is 2–3.[24] The prospects for using NaY to capture CO_2 were investigated and found to be reasonably promising.[9] The more hydrophobic NaY structure had fewer cations than did NaX, and the heat of adsorption for CO_2 was lower. Galhotra *et al.* studied CO_2 adsorption in zeolite Y, varying the cation type and water content.[94] Infrared spectroscopy data showed that most CO_2 molecules were physisorbed; however, some chemisorbed CO_2 was detected. Harlick and Tezel measured the CO_2 adsorption isotherms for NaY at different pressures [0.5–202 kPa] and temperatures [293–473 K]. The collected data were well represented as a Toth isotherm.[95]

Shao *et al.*[96] studied CO_2 and N_2 adsorption in NaY over a wide range of temperatures, from 303 K to 473 K, and at pressures up to 100 kPa. They found that the adsorptive uptake of CO_2 by the NaY was higher than in any other porous material reported, suggesting that NaY is a good adsorbent for CO_2 capture at high temperatures. The intensity of the interactions between CO_2 and the walls of the cavities in the zeolite were heterogeneously distributed. Maurin *et al.*[97,98] combined GCMC simulations with adsorption measurements on LiY and NaY (FAU) zeolites at various temperatures. A new FF for the Li^+-CO_2 interaction was derived based on *ab initio* calculations. Two types of adsorption behavior were observed for NaY and LiY zeolites at 323 K and 373 K. Ghoufi *et al.*[99] studied the adsorption of CO_2, CH_4, and an equimolar mixture in NaY by combining GCMC simulations with volumetric and gravimetric uptake experiments. The simulations showed a high CO_2-over-CH_4 selectivity in NaY across the range of pressures studied, revealing preferential adsorption sites for both adsorbates. Plant *et al.*[100] carried out both GCMC and MD simulations to study CO_2 adsorption in NaX and NaY (FAU). A new FF for the Na^+–CO_2 interaction was derived using quantum calculations. Two types of adsorption behavior were observed for NaY and NaX.

Plant *et al.*[101] carried out MD simulations to study the cation rearrangement in NaX and NaY (FAU) during the process of CO_2 adsorption. GCMC simulations, combined with microcalorimetry measurements, were performed by Maurin *et al.*[98] to study the interaction of CO_2 with two types of FAU surface. Plant *et al.*[102] combined quasi-elastic neutron scattering (QENS) with MD simulations to investigate CO_2 dynamics in LiY and NaY (FAU), where the transport diffusivity (D_T) was shown to increase with loading, whereas self-diffusivity (D_s) decreased. In addition, the authors showed that LiY exhibited significantly slower CO_2 self-diffusion due to the initial strong interactions between Li^+ cations and the adsorbate molecules.

The adsorption of CO_2 on HY (FAU, Si/Al = 8) was investigated by Pulido *et al.*[103] in a combined study of variable-temperature IR spectroscopy and DFT/coupled cluster (CC) calculations. The calculations showed that weak interactions played an important role in adsorption. The calculated and experimental stretching frequencies were in good agreement. The adsorption of CO_2 in the alkali-exchanged zeolite Y (Li^+, Na^+, K^+, and Cs^+) was investigated using DFT calculations (Plant *et al.*[104]). The cation–CO_2 geometry was investigated as a function of the nature of the alkali cations. The calculated adsorption enthalpies showed a decrease from Li^+ to Cs^+ and reproduced experimental microcalorimetry results. Chatterjee and Iwasaki[105] investigated the separation of gas components from a mixture of CO_2, N_2, CH_4, C_2H_6, and SF6, with a focus on the selective permeation of CO_2 from a mixture of CO_2/N_2 through a NaY membrane. Reactivity descriptors and interaction energies were calculated using DFT. Permeation, as a function of the affinity between gas molecules and the membrane wall, was analyzed to predict the optimal affinity strength (higher selectivity) for CO_2. Their results predicted the experimentally observed selective permeation order of $C_2H_6 < CH_4 < SF_6 < CO_2 < N_2$.[106]

Zeolite A (Fig. 1b) has small interconnecting windows composed of 8-rings. The small windows render zeolite A suitable for molecular sieving. The Ca^{2+} form of zeolite A is called 5A or CaA, the Na^+ form is called 4A or NaA, and the K^+ form is called 3A or KA, where the number corresponds to the approximate molecular window size. It is worthwhile comparing these sizes with the effective kinetic diameters given in Table 3. In an early seminal study, Breck *et al.* showed that the capacity for CO_2 adsorption varied with the Na^+/K^+ ratio in zeolite A (Fig. 3).[10] CaA had the largest heat of adsorption for CO_2 among the solid–CO_2 pairs studied by Harlick and Tezel.[9] The large heat is related to the very small pore size, the properties of Ca^{2+}, and the large number of aluminium atoms present in the structure. Zeolite A was shown to have an overall capacity for CO_2 sorption at 393 K that was lower than the capacity of NaX. The capacity loss was attributed to a stronger tendency toward forming chemisorbed carbonate species in zeolite A. The capacity of CaA was even lower than that of NaA.

Liu and Yang[107] used GCMC to study the adsorption of supercritical CO_2 on two types of zeolite with identical chemical

Table 3 Kinetic dimensions in zeolite

Gas	Kinetic dimension/nm
CO_2	0.33 [a]
N_2	0.365
CH_4	0.38

[a] Different values in the literature.

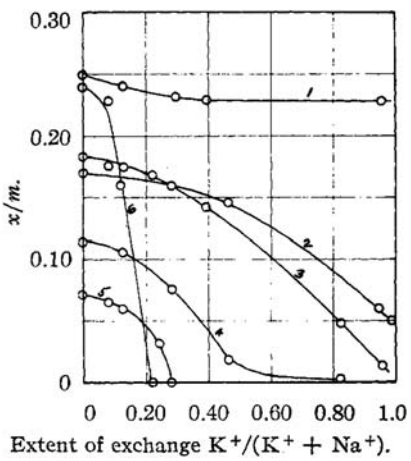

Fig. 3 From Breck *et al.*,[10] the uptake of different gases in NaKA: (1) water at 298 K and 0.6 kPa; (2) methanol at 298 K and 0.5 kPa; (3) CO_2 at 298 K and 93 kPa; (4) ethylene at 298 K and 93 kPa; (5) ethane at 298 K and 93 kPa; (6) O_2 at 90 K and 93 kPa. Reprinted with permission.

compositions but different pore structures, NaA and NaX. Jaramillo and Chandross[108] developed FFs for calculating the adsorption of NH_3, CO_2, and H_2O on NaA by GCMC. They also studied the geometry of the adsorption sites and correlated the loading with geometry. At low pressures, the adsorption geometry of CO_2 molecules was such that the longitudinal axis was directed toward the center of the supercage. At higher pressures, the two oxygen atoms were found to be equidistant from the Na^+. Akten *et al.*[109] used GCMC simulations to assess the adsorption selectivity of CO_2/N_2 and CO_2/H_2 mixtures as a function of temperature and gas composition. At room temperature, NaA showed a strong selectivity for CO_2 over both N_2 and H_2. The selectivity decreased slightly at high pressures. Ideal adsorption solution theory (IAST) predicted the adsorption selectivity at low partial pressures of CO_2 using a functional form that accurately described the isotherm for CO_2. IAST was found to perform reasonably accurately in modeling these adsorbed mixtures. Izumi *et al.*[110] precisely evaluated the window shrinkage of NaA, at a resolution of 0.01 nm, by calcination, rehydration, partial K^+ exchange, and low-temperature adsorption. The oxygen selectivity in a binary O_2/N_2 system and the CO_2 selectivity in a binary CO_2/N_2 were studied by MAS-NMR, single crystal X-ray diffraction (SCXD), and MD simulations. We recently showed that a high CO_2-over-N_2 selectivity could be achieved by carefully tuning the Na^+/K^+ ratio in zeolite A.[111]

All-silica microporous materials (or zeolites with very large Si/Al ratios) are hydrophobic, and hence much less sensitive to water adsorption than are aluminium-rich zeolites. This property has prompted many recent investigations into their ability to separate CO_2/CH_4 and CO_2/N_2 gas mixtures. CO_2 sorption on ZSM-5 and silicalite[112] (Fig. 1c) have been studied for this purpose.[8,9,113–115] ZSM-5 and silicalite have the structural code MFI and have intersecting channels with 10-membered rings.[85] These materials permit unhindered access to the porous network for all molecules relevant to CCS processes. It is instructive to see the apertures of the windows with the kinetic diameters listed in Table 3. The silicalite material contains no cations, and the heat of adsorption for CO_2 was determined to be small (27 kJ mol^{-1}).[113]

Previous studies measured the binary adsorption isotherms of CO_2, N_2, and methane on a ZSM-5 sorbent with SiO_2/Al_2O_3 ratios of 30 and 280.[114,115] Hirotani *et al.*[116] studied the adsorption of CO_2 in silicalite and NaZSM-5 using GCMC and found good agreement between the calculated adsorption isotherms and the experimental results collected by Yamasaki *et al.*[117] and Geiger *et al.*[118] The adsorption energy for NaZSM-5 was attributed to the electric field of the sodium cations. Zukal *et al.*[119] measured the adsorption isotherms of CO_2 in cation-exchanged (Li^+, Na^+, K^+, Cs^+) MCM-22, with varying molar ratios of Si/Al and at different temperatures. They calculated the isosteric heats of adsorption to gain insight into the interaction of CO_2 with alkali metal cations. GCMC simulations were carried out by Leyssale *et al.*[120] to study the thermodynamic properties of CO_2 and CH_4 adsorbed on the siliceous forms of MCM-22 and ITQ-1 (MWW), with their two independent pore systems. ITQ-1 was found to be CO_2-selective in CO_2/CH_4 mixtures, with a maximum in selectivity observed at low temperatures, high pressures, and CH_4-rich gas compositions. Yue and Yang[121] studied the adsorption and diffusion of binary mixtures of supercritical CO_2 and benzene on silicalite using GCMC and MD simulations. Their simulation results suggested that supercritical CO_2 fluid could be used to efficiently desorb larger aromatics in the zeolitic materials. MD simulations revealed that the large adsorbed benzene molecule had a pronounced effect on the diffusion of CO_2. Papadopoulos *et al.*[122] carried out coherent QENS experiments and MD simulations to study the concentration dependence of N_2 and CO_2 transport diffusion in silicalite-1. Sorbate–sorbate interactions were found to be much more attractive in CO_2/silicalite-1 than in N_2/silicalite-1. GCMC simulations of the adsorption of CO_2 and N_2 were carried out by Himeno *et al.*[123] on all-silica DDR (Fig. 1d) and MFI (Fig. 1c). The simulated sorption capacities, isosteric heats of adsorption, and Henry's constants, for all-silica DDR and MFI, agreed well with the experimental data.

García-Pérez *et al.*[124] studied the adsorption properties of CO_2, N_2, and CH_4 in all-silica microporous materials using molecular simulations. They computed the adsorption isotherms at a wide range of pressures and temperatures, and for pure (single-component), binary, and ternary component mixtures with varying bulk compositions.

A shortcoming of membranes is that they typically cannot possess both high adsorption and high diffusion selectivity. However, there are exceptions: for example, DDR membranes. Jee and Sholl[125] used MD simulations to study the diffusion of CO_2, and a transition state theory-based kinetic Monte Carlo scheme to accurately describe the extremely slow diffusion of CH_4 (less than 10^{-7} cm^2 s^{-1}, which is beyond the reach of MD) inside all-silica DDR ($Si_{120}O_{240}$) applying an improved FF, yielding results that agreed well with experiments.[126,127] They observed that the characteristics of CO_2/CH_4 diffusion in DDR were different from the characteristics of diffusion in nanoporous materials. In DDR, the diffusion rates of CO_2 were only weakly affected by the presence of the much slower-diffusing CH_4. They claimed that this unusual phenomenon related to different adsorption sites and diffusion mechanisms of the two species. In DDR, the 8-membered rings (8MR, 0.36×0.44 nm) and the 19-hedra cages ($\sim$0.6 nm) are the structural features that are relevant for molecular transport and adsorption. The 8MR are the most energetically favorable adsorption sites for CO_2; CO_2 adsorbs in the 19-hedra cages only after the 8MR are occupied. However, CH_4 can only occupy the larger 19-hedra cages. The adsorption of CO_2 in the 8MR hinders the hopping of CH_4 through the 8MR windows into the 19-hedra cages. Competitive adsorption of CO_2 and CH_4 occurs only in the 19-hedra cages. The large pore size ensures that CO_2 diffusion will not be impeded significantly by CH_4. The diffusive transport of CO_2 is only weakly affected by the presence of CH_4, while the more rapidly diffusing CO_2 molecules retard the slowly diffusing CH_4 molecules. Accordingly, they suggested a modified IAST, which describes the adsorption of mixtures of CH_4 and CO_2 in the 19-hedra cages of DDR and predicts the total adsorbed amount of CO_2 by adding the adsorbed CO_2 in the 8MR windows directly from the single-component data. It proved to perform better than the conventional IAST for this gas mixture. The combination of rapidly diffusing CO_2 and slowly diffusing CH_4 in DDR makes tit attractive for membrane-based or kinetically driven adsorption separations. The difference in diffusivities can enhance the adsorption-based selectivity of DDR for CO_2 relative to CH_4.

Krishna and van Baten[128] used GCMC and MD simulations to screen 12 microporous zeolitic structures to determine which membrane structure yielded the best selectivity for CO_2 separation from CH_4. They found that CHA and DDR, which have cages separated by narrow windows, provided the best selectivity with respect to permeation. Selassie *et al.*[129] performed atomistic MD simulations of the diffusion behavior of CO_2 and N_2, as both single components and as binary mixtures, in three all-silica microporous structures that contained variations in the pore structure: ITQ-3 (ITE; 8-ring), silicalite (MFI; 10-ring), and ITQ-7 (ISV; 12-ring). CO_2 consistently diffused more slowly than did N_2; however, the behavior within ITQ-7 and silicalite was found to differ from that within ITQ-3.

Krishna and van Baten[130] studied the separation of CO_2 from gaseous mixtures containing CH_4, N_2, or Ar in cage-type all-silica microporous solids (DDR, CHA, LTA, and ERI). All of these microporous solids contained 8-ring structures separated by narrow windows, and the selectivity for CO_2 separation was found to be dictated by both the adsorption and diffusion characteristics. Their GCMC simulations showed that a much higher proportion of CO_2 was present in the window regions of cage-type structures than was present within the cages themselves. MD simulations of self-diffusion in binary mixtures showed that CO_2 slowed the diffusion of the partner molecules to a much greater degree than that predicted by Maxwell–Stefan (MS) diffusion theory, parameterized by pure component data. GCMC and MD simulation results suggested that DDR and CHA should yield high permeation selectivities for membrane-based separation in CO_2/CH_4, CO_2/N_2, and CO_2/Ar mixtures. For N_2/CH_4 separation, DDR and FRI were found to be good choices.

Krishna and van Baten reported the results of GCMC simulations[131] for the adsorption of CO_2/CH_4, CH_4/N_2, and CO_2/Ar mixtures in DDR structures, and observed that the window regions contained essentially no CH_4 or Ar. These molecules were predominantly adsorbed within the cages, whereas CO_2 and N_2 molecules were adsorbed both within the cages and in the window regions. MD simulations showed that those CO_2 molecules adsorbed strongly at the windows, which hindered inter-cage diffusion of other components in the mixtures. MS theory did not describe this effect.

Krishna *et al.*[132] carried out MD simulations to estimate the dependence of MS CH_4 and CO_2 diffusivity on loading, within three structural topologies characterized by: (i) intersecting channels, (ii) one-dimensional channels, and (iii) cages separated by windows. Krishna *et al.*[133] performed MD simulations to determine D_S for CH_4 and CO_2, for both pure components and in 50–50 mixtures, over a range of molar loadings in MFI, CHA, and DDR structures. They found that the inter-cage hopping events of molecules in CHA and DDR structures, in which the cages were separated by narrow windows, were practically independent of one another; consequently, the diffusivities of pure components were the same as those in the mixture. However, in MFI, which contained intersecting channels, species that are more mobile diffused significantly slower in the mixture. Van den Bergh *et al.*[134] introduced a new model, the "relevant site model", to describe the dependence of diffusion in zeolites on loading. This model assumed that segregated adsorption in cage-like zeolites, within the MS framework for mass transport, described diffusivity data for N_2 and CO_2 in DDR[135] (8-ring and cage-like all-silica structure) very well up to saturation. They also successfully extended the model to non-isothermal diffusivity data from CO_2 and N_2 in the DDR all-silica structure. Ohta *et al.*[136] performed dynamic Monte Carlo (DMC) simulations to estimate the perm-selectivity of binary mixtures (CO_2/N_2) in zeolite-like porous membranes using several hypothesized porous structures. The rates of hopping between different adsorption sites, estimated using an empirical atomistic FF, were used to parameterize the DMC simulations. The simulation times permitted by DMC were much longer than those permitted by conventional MD simulations were. Goj *et al.*[137] studied the adsorption of CO_2 and N_2, as both single components and as binary mixtures, in three all-silica structures with different pore structures (silicalite, ITQ-3, and ITQ-7) using atomistic MC simulations. All of the all-silica materials were found to preferentially adsorb CO_2 over N_2 in single-component and in mixture adsorption studies. The observed CO_2-over-N_2 selectivity varied strongly with changes in the crystal structure. The highest selectivity was found for ITQ-3.

Many zeolites occur in nature, some of which have been tested for CO_2 adsorption. Clinoptilolites are examples of such natural zeolites. They are typically relatively hydrophobic, have a high Si/Al ratio, and are known to be good SO_2 sorbents.[138] Aguilar-Armenta *et al.* studied the equilibrium and kinetic uptake of CO_2, N_2, and CH_4 in clinoptilolites.[139] CO_2 sorption and selectivity in Mordendite (MOR) was studied at high pressures. The selectivity for CO_2-over-N_2 adsorption was found to be higher in the protonated than in the sodium form, thought to reflect the weaker affinity for N_2 adsorption in the protonated form.[54] Siriwardane *et al.* showed that most CO_2 was physisorbed, and that high sodium content promoted a high uptake of CO_2.[140]

2.2 Aluminium phosphates

Microporous aluminophosphates ($ALPO_4$) and silicoaluminophosphates ($SAPO_4$), with structures and properties similar to those of zeolites, were developed by Flanigen and coworkers.[141,142] The overall framework of the $ALPO_4$ materials was neutral; however, the variations in the electric field gradients were significant, and the interaction between this material and CO_2 was strong and exothermic. CO_2 adsorption in $ALPO_4$-5 (AFI) was measured by Martin *et al.*[57] The measured adsorption capacity for CO_2 was large for $ALPO_4$-14 (AFN).[58] The $SAPO_4$ framework was negatively charged and required cations for overall charge balance. After exchanging the cations with strontium, $SAPO_4$-34 (CHA) showed significantly enhanced adsorption properties for CO_2 at pressures that were low relative to the structure containing Na^+ and Ag^+ ions.[59] SAPO-34 is a candidate material for membranes or kinetic adsorbents for CO_2/CH_4 separation.

Deroche *et al.*[60] investigated the adsorption properties of CO_2 in $SAPO_4$ STA-7 (SAV) in a combined GCMC and microcalorimetry study. Newly derived interatomic potentials were used to describe the interaction between CO_2 and the Brønsted acid sites, yielding good agreement with experimental data. One method for enhancing CO_2 adsorption in $ALPO_4$ and $SAPO_4$ materials achieved additional alkalinity by introducing nitrogen atoms. The number of basic sites in the modified $SAPO_4$-34 was found to

be correlated with the number of nitrogen atoms present.[143] We anticipate continued experimental and theoretical treatment of CO_2 adsorption and selection in $ALPO_4$ microporous solids. These materials are less hydrophilic than zeolites, may be synthesized with a variety of structures, and have yet to be extensively investigated for this purpose.

2.3 MOFs

MOFs are porous structures with very large pore sizes, composed of both inorganic and organic building blocks. MOFs are crystalline materials that commonly feature interconnected pores and are composed of a metal ion coordinated by a relatively rigid organic linker. Two representative MOFs are presented in Fig. 4. After their discovery, these materials generated considerable attention in the literature. Several excellent reviews provide introductions to these materials.[144–148] Düren *et al.*[149] gave a useful, short tutorial review describing the application of molecular simulations to predictions of the adsorption behavior of MOFs. They described the molecular-level insights that may be gained from characterizing the adsorption properties of metal–organic frameworks.

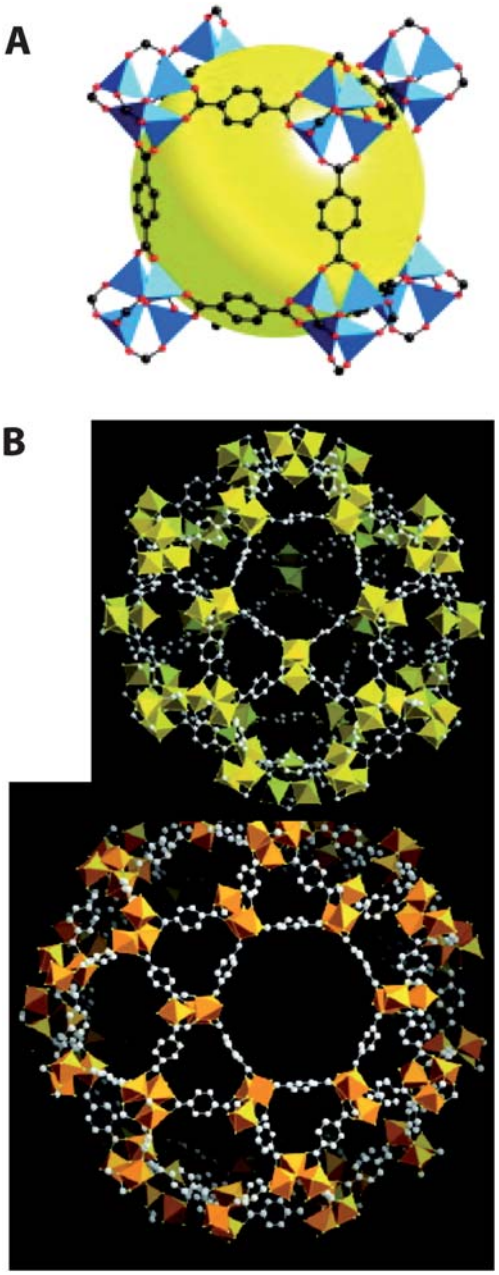

Fig. 4 Two representative MOFs. (A) IRMOF-1 or MOF-5;[150] (B) MIL-101 with its large and small pores.[12] Redrawn with permission.

2.3.1 Zn-based MOF. Yaghi and coworkers synthesized and studied the sorption properties of CO_2 and N_2 (among other gases) in a range of MOFs.[11,61,62,144,150–152] MOF-177 showed a very high capacity for adsorbing CO_2 at partial pressures above 1.5 MPa (Fig. 5); however, the capacity was low at small CO_2 pressures.[11] The coordinating metal ion was Zn^{2+}, and the organic linker was the benzene 1,3,5-tribenzoate group. The observed sigmoidal shape of the adsorption isotherm, for MOF-177 and similar MOFs, is still under scientific discussion.

Walton *et al.*[33] demonstrated that the shapes of the adsorption isotherms of CO_2 in IRMOF-1 could be predicted by molecular simulations using a rigid crystal structure. They claimed that the sorbate–sorbate electrostatic interactions were essential for predicting the inflections and steps of the adsorption isotherms. The adsorption equilibrium and diffusion of CO_2 on microporous metal–organic framework crystals (MOF-5, or IRMOF-1) were studied by Zhao *et al.*,[153] the Freundlich adsorption isotherm equation can fit well the CO_2 adsorption, and MOF-5 (Fig. 4a) was found to be an attractive adsorbent for separation of CO_2 from flue gas.

Yang *et al.*[154] performed GCMC simulations of CO_2/H_2 mixtures to study gas separation in three pairs of isoreticular metal–organic frameworks (IRMOFs), with and without catenation, at room temperature. They found that CO_2 selectivity in the catenated MOFs with multi-porous frameworks was much higher than that in the non-catenated MOFs. The electrostatic interactions appeared to be important for selectivity, even qualitatively changing the adsorption behavior and playing a dominant role, particularly at low pressures. Liu *et al.*[155] performed a systematic molecular simulation of three pairs of IRMOFs to compare the adsorption separation selectivity of

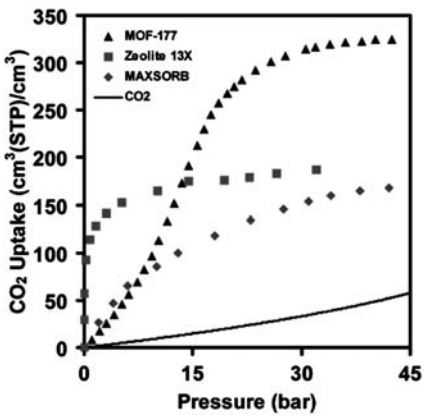

Fig. 5 Uptake of CO_2 on MOF-177 as compared with zeolite X, porous carbon (MAXSORB), and pressurized CO_2.[11] Reprinted with permission.

these MOFs in the presence of CH_4/H_2 mixtures. They showed that the CH_4 selectivity in the interpenetrated IRMOFs was greatly enhanced relative to the noninterpenetrated IRMOFs, due to the formation of additional small pores and adsorption sites in the interpenetrating frameworks. The authors showed that IAST was likely to be applicable, even to interpenetrated MOFs with complex structures.

Bastin *et al.*[156] examined a microporous MOF Zn(BDC)(4,4′-Bipy)$_{0.5}$ (MOF-508b, BDC = 1,4-benzenedicarboxylate, 4,4′-Bipy = 4,4′-bipyridine) for the separation and removal of CO_2 from binary CO_2/N_2 and CO_2/CH_4, and ternary $CO_2/CH_4/N_2$ mixtures, providing the first reported use of microporous MOFs for the separation and removal of CO_2 from binary and ternary mixtures using fixed-bed adsorption. Barcia *et al.*[157] studied the adsorption of CO_2, N_2, and CH_4 on crystals of MOF-508b, at temperatures in the range 303–343 K and at partial pressures up to 450 kPa. MOF-508b was found to be very selective for CO_2, and the loadings of CH_4 and N_2 were practically temperature-independent. The Langmuir isotherm model provided a good representation of the equilibrium data. A dynamic model based on the linear driving force (LDF) approximation for mass transfer was used to describe the adsorption kinetics of single, binary, and ternary breakthrough curves with good accuracy. The LDF model has been successfully tested (in previous studies[158,159]) in simulations of the breakthrough curves for alkanes in zeolitic materials. The set of equations was solved numerically using the orthogonal collocation method. The intra-crystalline diffusivity of CO_2 was found to be an order of magnitude faster than the intra-crystalline diffusivities of CH_4 or N_2.

Zeolitic imidazole frameworks (ZIFs) have structures formed by heterocyclic and nitrogen-containing linkers with topologies very similar to those of zeolites. Metals play a similar role on ZIFs to that of Si and Al atoms on zeolites, by mainly contributing with electrostatic interactions, the vdW contributions can be ignored. This fact makes ZIFs substantially different from other MOFs.

Using high-throughput experimental techniques, Yaghi and coworkers identified a range of candidate materials with a high capacity for CO_2 adsorption.[61,62,152] Liu *et al.*[160] developed a FF to describe the framework atoms of two typical ZIFs, ZIF-68 and ZIF-69. They used this FF in a combined GCMC and MD simulation study to investigate the adsorption and diffusion behavior of CO_2 in ZIFs. Their results showed that the small pores in ZIF-68 and ZIF-69 provided preferential adsorption sites for CO_2 molecules. Rankin *et al.*[161] computed the adsorption and diffusion properties of CO_2, N_2, CH_4, and H_2 in ZIF-68 and ZIF-70 using atomistic simulations. The simulated adsorption and diffusion of the quadrupolar molecules depended dramatically on the atomic charges used. The agreement between simulations and experiments[152] for the N_2 adsorption isotherms in ZIF-68 and -70 was very good when charge–quadrupolar interaction terms were included, whereas simulations over-predicted the amount of CO_2 adsorbed at 298 K if these terms were dropped.

Babarao *et al.* reported an MC/MD simulation study for upgrading natural gas (CO_2/CH_4, CO_2/N_2 mixtures) in rho zeolite-like metal–organic frameworks (rho-ZMOF).[162] CO_2 was preferentially adsorbed relative to CH_4, N_2 due to the strong electrostatic interactions of CO_2 with the ionic framework and Na^+ ions. At ambient temperature and pressure, the CO_2 selectivities were 80 for the CO_2/CH_4 mixture, and 500 for the CO_2/N_2 mixture. In particular, they described the effects of water for the separation of CO_2/CH_4 mixture on this material.[163] They found that the selectivity decreased by one order of magnitude with a trace amount of H_2O added into CO_2/CH_4 mixture.

Debatin *et al.* synthesized another microporous zinc–organic framework rescently by *in situ* synthesis of an imidazolate-4-amide-5-imidate ligand; this sorbent was shown to have a very high CO_2 uptake.[64]

2.3.2 MIL. Chromium and aluminium ions can be used as the coordinating metals in MOFs. Llewellyn and coworkers studied the uptake of CO_2 in a series of MOFs, in which Cr^{3+} and Al^{3+} had been substituted at the coordinating cation positions.[63] The Materials Institute of Lavoisier (MIL) solids have been shown to yield large CO_2 uptakes. In particular, MIL-100 and MIL-101 (Fig. 4b) showed very high capacities for CO_2 adsorption at high pressures.[12]

In particular, MIL-53 shows "breathing" phenomenon upon temperature change or host–guest interactions. Such flexible and dynamic frameworks are interesting as they open potential applications for high-performance molecular recognition and high selectivity for guest inclusion and release.

Based on the partial charges of the framework derived from DFT calculations,[42] Ramsahye *et al.* performed a GCMC simulation to compare the CO_2 adsorption mechanisms at work in two members of the MIL-*n* family of hybrid metal–organic framework materials, MIL-53 (Al) and MIL-47 (V).[46,47] A structural transition between large-pore and narrow-pore forms was observed in MIL-53 (Al) around 600 kPa, although this transition was not seen for MIL-47 (V). They derived a "composite" absolute isotherm from the calculated CO_2 adsorption isotherms by applying the X-ray diffraction structures of MIL-53np (Al) (narrow pore) and MIL-53lp (Al) (large pore) respectively. They found it to be comparable to experimental data collected by microcalorimetry. The "composite" differential enthalpy of adsorption agreed reasonably well with experimental results. At low CO_2 loadings, snapshots from GCMC showed typical pore-bridging double interaction (Fig. 6), O_{CO2}–$H_{\mu 2\text{-}OH}$ distances of 0.198 and 0.176 nm, which is only

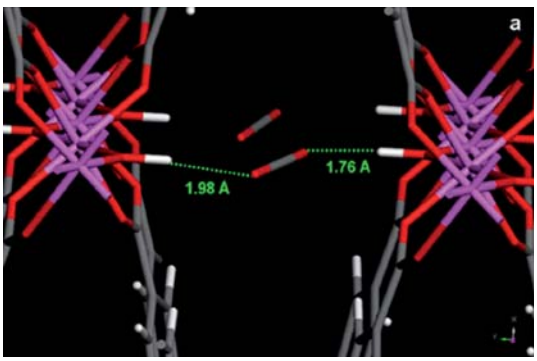

Fig. 6 From Ramsahye *et al.*[46] The double interaction, the most prevalent for the Al-containing structure at a CO_2 loading of 2 molecules per unit cell (u.c.).

possible in the narrow pore MIL-53 (Al). At high loadings, the reach of the saturation capacity of the MIL-53np (Al) leads to an increased level of intermolecular interactions between CO_2 molecules and break the pore-bridging geometry and weaker adsorbate–adsorbent interaction geometries are formed. They argued that this was likely to be ultimately responsible for a transition from the narrow pore structure to the large pore version. Those adsorption geometries were confirmed in a comprehensive DFT study by the same group.[164] The lack of μ_2-OH groups within the pore of MIL-47 (V) makes it a homogeneous adsorbent for CO_2, thus no "breathing" effect is observed.

Salles *et al.*[35] used MD simulations to study the thermal activation and guest-induced structural transformations of MIL-53 (Cr).[165] Capture of the two-step structural switching, induced by CO_2 adsorption in the Cr-containing framework at finite temperatures, was shown to be successful. They found that the proper parameterization of the bonded interaction within the framework was important in reproducing the breathing process. The inorganic node was described by a Cr–O bonded intramolecular term and nonbonded Lennard-Jones (LJ) interactions. An additional torsion term ($Cr–O_{carboxyl}–C_{carboxyl}–O_{carboxyl}$) was also included for interactions between the inorganic and organic parts. With energy minimization, they confirmed bistable behavior of the large-pore and narrow-pore structures observed by experiment, with only 5 kJ mol^{-1} per formula unit in favor of the large-pore structure. The simulated vibrational frequencies for the MIL-53 (Cr) framework were in good agreement with infrared data. They also calculated that a transition from the narrow-to-large-pore structure could be thermally activated at a temperature above 600 K. Starting with the bare large pore structure from XRPD data, with loading of different number of CO_2 molecules per cell, they performed a series of NσT ensemble MD simulations at 300 K, and derived the unit cell volumes evolution with MD simulation time. From the final equilibrated cell volumes, the evolution of the unit cell volume of MIL-53 (Cr) as a function of the CO_2 loading was derived. Their calculations predict the predominance of the large-pore form at very low loading and above 5.2 CO_2 per u.c., whereas the narrow-pore version was present in the intermediate domain of loading, within the same range as that obtained from *in situ* XRPD and manometry experiments. From the MD snapshots, within the narrow-pore channels, the CO_2 molecules were aligned along the direction of the tunnel, parallel to each other, leading to a double interaction [$O_{CO_2}–H_{\mu 2\text{-OH}}$ and $C_{CO_2}–O_{\mu 2\text{-OH}}$] with the μ2-OH groups present at the pore wall. The geometries were in good agreement with the *in situ* XRPD analysis[165] and the DFT calculations[164] (Fig. 7). By using the modified FF, they simulated the transport diffusivity of CO_2 in MIL-53 (Cr).[36] It was the first time to combine QENS experiments and MD simulations to follow the transport diffusivity of a guest molecule confined in a highly flexible MOF-type material characterized by a spectacular phase transition between two distinct structural forms.

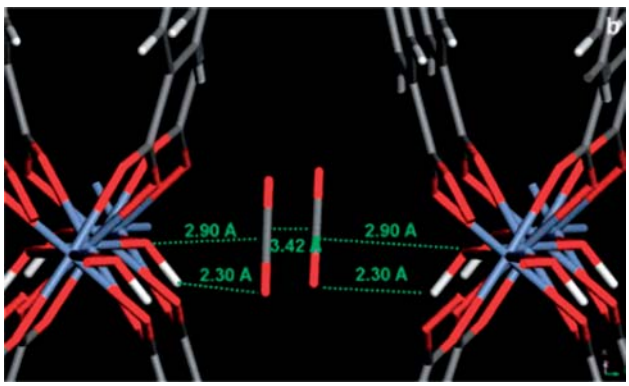

Fig. 7 From Ramsahye *et al.*[46] Arrangement of 2 CO_2 molecules in a MIL-53np (Cr) calculated from DFT.

Coombes *et al.*[166] carried out DFT and FF-based calculations to model the "breathing" of MIL-53(Cr) in both its large- and narrow-pore forms. They found that the sorbate-free large-pore structure appeared to be the global minimum. Their calculations, in which water molecules were introduced into the structures, illustrated the physisorption-driven pore breathing process, in which water molecules in the narrow-pore form were more strongly stabilized. Hammon *et al.* studied binary adsorption of CO_2 and CH_4 in MIL-53(Cr), and discussed the possibility of using this MOFs for the pressure swing-driven separation of CH_4 and CO_2.[167]

2.3.3 Cu-based MOF. Yazaydin *et al.*[168] used molecular simulation techniques to predict that CO_2 uptake and selectivity with respect to N_2 and CH_4 in the Cu-BTC MOF were significantly increased by the presence of water molecules coordinated to open metal sites in the framework. The same authors later confirmed this prediction experimentally. Yang *et al.*[169] performed a GCMC simulation of the adsorption and separation of CO_2 from flue gases (mixtures of $CO_2/N_2/O_2$) in Cu-BTC MOF, and found this a promising material for separating CO_2 from flue gases. Keskin *et al.*[32] studied gas adsorption and diffusion in Cu-BTC on the atomic level to predict the performance of Cu-BTC membranes for the separation of H_2/CH_4, CO_2/CH_4, and CO_2/H_2 mixtures. They found this membrane to have higher selectivities for all three mixtures than did MOF-5 membranes. Liang *et al.* experimentally studied Cu-BTC for its potential for CO_2 separation, and determined the isotherms for CO_2, CH_4, and N_2 at various pressures and temperatures. The authors observed a quadrupled capacity for CO_2 adsorption compared with NaX. Cu-BTC was shown to be unstable at moderate temperatures and humid conditions.[170] Cheng *et al.* studied a specific Cu-MOF, revealing a CO_2-gate adsorption mechanism for humid gas.[171]

Based on studies using a combined computational methodology, MD and GCMC simulations, DFT calculations, and TST, Watanabe *et al.*[17] predicted that the MOF Cu(hfipbb)(H_2hfipbb)$_{0.5}$ would have a very high selectivity in the kinetic membrane-based separation of CO_2/CH_4 mixtures. It contains cages (~5.1 × 5.1 Å) connected by small windows (~3.5 × 3.2 Å). This structure feature makes this microporous MOF an equally promising material as DDR[125] and SAPO-34[59] for CO_2 -over- CH_4 separations.

2.3.4 Others. Iron-coordinated MOFs (IRMOP-51) adsorbed significant amounts of CO_2 at low pressures.[151] A Sc^{3+}-containing MOF was shown to adsorb only small quantities of CO_2 (1 mmol at 100 kPa and 303 K).[172]

2.3.5 Adsorption capacity/selectivity comparison studies among zeolites and MOFs. A comparison of the separation of mixtures of CO_2/N_2 and CH_4/N_2 was systematically studied using molecular simulations by Liu and Smit, using two classes of nanoporous materials, microporous silicates, and MOFs.[29] Three microporous silicates (MFI, LTA, and DDR) and seven MOFs (Cu-BTC, MIL-47 (V), IRMOF-1, IRMOF-12, IRMOF-14, IRMOF-11, and IRMOF-13) were considered. To validate the FFs, both adsorption selectivity and pure CO_2 and CH_4 adsorption isotherms were calculated. The MOFs appeared to have higher capacities for gas adsorption than the other kinds, although both kinds yielded similar gas separation performances. When the preferred gas component was characterized by a large quadrupole moment, both silicates and MOFs enhanced the separation selectivity.

Atomistic GCMC simulations were carried out by Babarao *et al.*[173] to study the adsorption capacities for pure CO_2, pure CH_4, and their binary mixtures (in silicalite, C-168 schwarzite, and IRMOF-1) at room temperature. Although IRMOF-1 had a significantly higher adsorption capacity than did either silicalite or C-168 schwarzite, the adsorption selectivity of CO_2 over CH_4 was found to be similar in all three adsorbents. A dual-site Langmuir–Freundlich equation was used to satisfactorily describe the isotherms. They also studied[174] the self-diffusion, corrected diffusion, and transport diffusion of CO_2 and CH_4 in silicalite, IRMOF-1, and C-168 schwarzite by MD simulations, and evaluated the activation energies at infinite dilution. An Arrhenius expression was employed to evaluate the energy from the observed diffusivities at various temperatures. The Maxwell–Stefan model predictions for self-diffusion, corrected diffusion, and transport diffusion for pure CO_2 and CH_4 agreed well with the simulation results. Based on the adsorption and self-diffusivity in the CO_2/CH_4 mixture, the permselectivity was found to be marginal in IRMOF-1, slightly enhanced in MFI, and greatest in C-168 schwarzite. Although IRMOF-1 had the largest storage capacity for CH_4 and CO_2, its selectivity was not satisfactory.

Babarao *et al.*[175,176] studied the adsorption and separation of CO_2/CH_4 mixtures using molecular simulations in a series of MOFs with unique characteristics, such as exposed metals (Cu-BTC, PCN-6′, and PCN-6), catenation (IRMOF-13 and PCN-6), and extra framework ions (soc-MOF). The exposed metals and catenation were found to slightly enhance the selectivity of CO_2 over CH_4. The extraframework ions NO_3^- in charged soc-MOF act as additional adsorption sites for quadrupolar CO_2 molecules, and the selectivity in soc-MOF was 1 order of magnitude higher than in IRMOFs and PCNs and the highest among various MOFs reported to date.

Farrusseng *et al.*[177] systematically studied the heats of adsorption of many adsorbates, including CO_2, CH_4, N_2 on a series of MOFs: IRMOF-1, IRMOF-3, and Cu-BTC, combining experiment and simulation. Simulations predict a large temperature dependence of the heat of adsorption in Cu-BTC, which is reduced significantly when the small pockets are blocked. Martin-Calvo *et al.*[178] used MC simulations to study the adsorption and separation of natural gas components in IRMOF-1 and Cu-BTC metal–organic frameworks. They estimated the adsorption isotherms of pure components, binary, and five-component mixtures. Their simulations indicated that though IRMOF-1 had a significantly higher adsorption capacity than Cu-BTC, the adsorption selectivity of CO_2 over CH_4 and N_2 is found to be higher in the latter, proving that the separation efficiency was largely affected by the shape, the atomic composition and the type of linkers of the structure.

Yang *et al.*[179] reported a systematic computational study of the effects of organic linker, pore size, pore topology, and electrostatic fields on the adsorption and diffusion behavior of CO_2 in nine typical metal–organic frameworks (MOFs). They showed that the high CO_2 adsorption capacity could be described as the complex interplay of these properties. The MOFs in this study showed higher CO_2 adsorption capacities than did either zeolites or carbon materials under practical conditions, and the most suitable pore size was found to be 1.0–2.0 nm. In addition, the D_S values for CO_2 in the MOFs were comparable to those observed in zeolites.

Keskin and Sholl[180] introduced an efficient approximate method for screening MOFs based on atomistic models that sped the computational time associated with models of membrane applications. They validated the model *via* comparison with detailed calculations of the permeation of CH_4/H_2, CO_2/CH_4, and CO_2/H_2 mixtures at room temperature through IRMOF-1 and Cu-BTC membranes. The model was then applied to six additional MOFs (IRMOF-8, -9, -10, and -14, Zn(bdc)(ted)(0.5), and COF-102) to estimate the effects of chemical diversity and interpenetration in MOF membranes on the separation of light gases.

Yazaydin *et al.*[34] screened 14 MOFs for CO_2 capture from flue gas at an operation pressure below 1 bar using a combined experimental and modeling approach (Fig. 8). They found that MOFs with a large adsorption capacity for CO_2 at high pressures often do not perform well at low pressures. IRMOF-1 and MOF-177 are among the lowest performing materials. Below 1 bar, CO_2 uptake correlates well with the heat of adsorption, thus MOFs having a high density of open metal sites are promising. They found that changing the metal from Zn in M\DOBDC (DOBDC = dioxybenzenedicarboxylate) to Mg, Co, or Ni provides large changes in CO_2 uptake. M\DOBDC have open metal sites that can interact with adsorbate molecules, and Mg\DOBDC performs particularly well. HKUST-1 (also known as Cu(BTC)), UMCM-150, and UMCM-150(N)$_2$ have lower density of open metal sites than M\DOBDC and perform not as

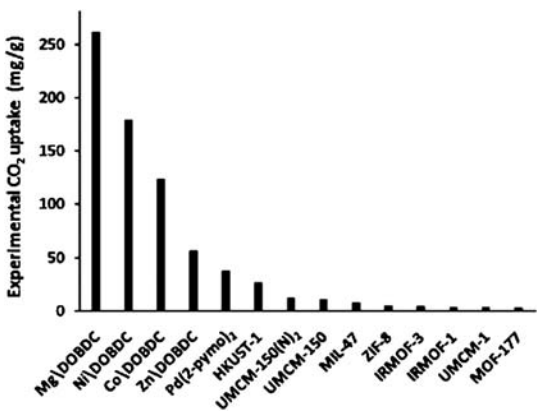

Fig. 8 From Yazaydin *et al.*[34] Experimental CO_2 uptake in screened MOFs at 10 kPa. Data obtained at 293–298 K.

well as M\DOBDC. The LJ parameters in their force field for the MOF atoms were taken from DREIDING or UFF force field. Partial charges were fitted from DFT cluster calculations. In spite of bad performance for strong interactions between open metal sites and CO_2, their model correctly predicted the top 5 MOFs: Pd(2-pymo)$_2$, Mg\DOBDC, Ni\DOBDC, Zn\DOBDC, and Co\DOBDC in agreement with the experiments.

2.3.6 Modification of MOFs and potential MOFs design. Modifications of the MOF frameworks were shown to successfully enhance the uptake of CO_2. Demessence *et al.* derived and studied the spectacular capacity for CO_2 uptake of a triazolate-bridged MOF functionalized with ethylenediamine.[181] Functionalization led to an imidazolate framework with a high capacity for sorption of CO_2. Bae *et al.* reported that the CO_2-over-N_2 selectivity could be significantly enhanced by replacing solvent molecules with certain highly polar ligands.[182] Wang *et al.* revealed that a post-synthetic covalent modification of a MOF structure could activate the "breathing" behavior upon adsorption of certain gases.[183] Bae *et al.*[184] studied the adsorption of CO_2 and CH_4 in a mixed-ligand MOF $Zn_2(NDC)_2(DPNI)$ [NDC = 2,6-naphthalenledicarboxylate, DPNI = N,N′-di-(4-pyridyl)-1,4,5,8-naphthalene tetracarboxydiimide] using volumetric adsorption measurements and GCMC simulations. From the single-component CO_2 and CH_4 isotherms, adsorption of the mixtures was predicted using IAST, and the applicability of IAST was validated with GCMC simulations.

The force field parameters of molecular mechanics for MOFs are often not available, because of the wide range of possible inorganic fragments involved. The generic force field like UFF and DREIDING are derived by a number of established rules from atomic parameters are usually used to describe the MOF framework. These parameters are usually not very accurate and the framework is usually kept frozen at the experimentally determined structure. It limits the applicability of molecular in screening and design of MOFs for with specific gas adsorption behaviors, especially when MOFs have flexible frameworks. High quality force field parameters are required to describe precisely the "breathing" mechanism involved in flexible MOFs.

Tafipolsky and Schmid[44] proposed an efficient, systematic strategy to parameterize a force field of molecular mechanics from first principles reference data by optimizing a novel objective function with a genetic algorithm. Due to the efficiency of this approach, it is possible to abandon the need for transferability of the parameters. It is a "bonded" force field, *i.e.*, bond stretching, angle bending, torsion and stretch–stretch, stretch–bend cross terms are also considered in the metal ion interacting with its surrounding atoms. Using this approach, the authors claimed that a database of force field parameters, suitable for molecular simulations of coordination polymers, and considering the framework flexibility, could be parameterized from different types of secondary building units and linkers. Applying this scheme to MOF-5, in a "building block" approach, parameters are derived for the two model systems, zinc formate ($Zn_4O(O_2CH)_6$), and dilithium terephthalate. Reference data were obtained from density functional theory. The resulting potential gives excellent agreement with the structure, vibrational frequencies, thermal behavior, as well as elastic constants for the periodic MOF-5. Because no experimental data were used in the parameterization, the method could possibly also be used for not yet synthesized systems and allow for screening of MOFs.

Aiming at the design of linker molecules, which could form parts of new MOFs with enhanced affinity for CO_2 adsorption at low pressure, Torrisi *et al.* studied interaction of CO_2 with functionalized benzenes using density functional theory. These moieties contained methyl groups, halogen substituents,[185] polar side groups substituents,[186] including $–NO_2$, $–NH_2$, –OH, $–SO_3H$, and –COOH. Halogen substituents have an electron-withdrawing effect on the aromatic ring, which destabilizes the π–quadrupole interaction between benzene and CO_2, thus have negative effect on CO_2 adsorption. Methyl groups, on the other hand, have a positive inductive effect, which strengthens the CO_2-aromatic interaction. They found that the best substituents were $–NH_2$, $–SO_3H$, and –COOH. Such polar groups can lead to a whole range of favorable configurations, where a variety of host–guest interactions are at play, including lone-pair electron donation, H-bond like interactions. In addition, they pointed out that in a nanoporous material, additional effects restrict the freedom for the gas molecules to diffuse away from sorption sites. Molecular confinement, such as binding to more than one ligand, CO_2–CO_2 interactions, *etc.*, could further serve to enhance the affinity for CO_2.

2.4 COFs and porous polymers

MOFs and zeolites are typically hydrophilic, and their applications toward CO_2 separation from flue gases necessitate a drying stage. To circumvent such drying, significant efforts have been devoted to identifying materials that do not contain hydrophilic cation sites. A variety of organic porous materials has been produced without metal ions, with good prospects for CO_2 separation. Choi *et al.* studied CO_2 sorption in a three-dimensional (3D) polymeric network.[187] NASA uses a hybrid material that contains polyethylenimine (PEI) bonded to a high-surface-area polymethylmethacrylate mixed with polyethylene glycol (PEG) for CO_2 capture during space travel.[188] Budd *et al.* described microporous materials made from soluble polymers,[189] and Ritter *et al.* studied the limits of microporosity for CO_2 sorption in certain polyimides.[190]

Covalent organic frameworks (COFs) are crystalline organic porous materials without metal ions. Furukawa *et al.* demonstrated high capacities for CO_2 adsorption in COFs, studying H_2, CO_2, and CH_4 adsorption in seven COFs over a range of pressures and temperatures. The studied COFs were COF-1, COF-5, COF-6, COF-8, COF-10, COF-102, and COF-103. COFs-102 and -103 showed very high CO_2-uptake capacities.[13]

CO_2 adsorption in COFs containing three-dimensional (3D) (COF-102, COF-103, COF-105, and COF-108), two-dimensional (2D) (COF-6, COF-8, COF-10), and one-dimensional (1D) (COF_NT) structures were estimated by Babarao and Jiang[191] using computer simulations. The dimensionalities of the COFs refer to the dimension of the channel systems of these sorbents. In this earlier work, COF-105 and COF-108 appeared to have exceptionally high adsorption capacities, surpassing even the capacity of MOF-177. The authors found molecular-based structure–function correlations useful for predicting capacity and for screening COFs for CO_2 adsorption. Yang and Zhong[192] carried out GCMC simulations to investigate the adsorption

properties of CO_2, CH_4, and H_2 in 2D COFs with varying pore sizes. They predicted a stepped behavior common in gas adsorption, in which multilayer formation was the underlying mechanism. In general, they observed that temperature, pore size, the strength of interactions between adsorbates, and the strength of interactions between adsorbates and adsorbents affected the properties of the stepped mechanism.

Barbarao and Jiang[193] reported a systematic molecular simulation study of CO_2 adsorption in a series of MOFs (IRMOF1, Mg-IRMOF1, Be-IRMOF1, IRMOF1-$(NH_2)_4$, IRMOF10, IRMOF13, and IRMOF14), as well as UMCM-1, a fluorous MOF (F-MOF1), and a covalent–organic framework (COF102). The authors concluded that the affinity of these adsorbents for CO_2 could be enhanced by the addition of functional groups. The pore size was also observed to constrict, *via* interpenetration of the framework, which simultaneously increased the isosteric heat and Henry's constant, yielding stronger adsorption at low pressures. The authors observed that the organic linkers played a critical role in determining the free volume and accessible surface area of the material, and the organic linkers largely determined the estimated CO_2 adsorption at high pressures. COF-102 was found to be a promising CO_2 adsorption candidate with a high adsorption capacity at very low pressures.

2.5 Carbons

Porous carbons have been investigated as potential CO_2 sorbents, revealing a distinct advantage over zeolites in terms of hydrophobicity. Still, the uptake of CO_2 was reduced by competitive adsorption of water onto the carbons.[194] Many types of porous carbons have been developed: activated carbons, carbon molecular sieves (CMS), carbon nanotubes (CNT), and more exotic constructs such as NanoBuds and graphene.

2.5.1 Activated carbons. Activated carbons are micro- and mesoporous solids, typically with a broad pore size distribution (PSD), which have found many commercial applications.[4,22] The adsorption properties of activated carbons are introduced *via* carbonization and physical or chemical activation. CO_2 sorption on activated carbons has been studied for a long time.[195] Walker *et al.*[196] compared CO_2 capture in activated carbons and in zeolite A, concluding that zeolites offered better CO_2 capture in space crafts, even though a two-stage system would be required to remove water. The kinetics of CO_2 adsorption have been studied in monolithic carbons by Ruthven *et al.*[197] Urbonaite *et al.* prepared porous carbons *via* the chlorination of metal carbides, and studied the adsorption of CO_2 on these materials.[198] At high pressures, activated carbons were shown to have higher CO_2-sorption capacities than do zeolites.[199]

Montoya *et al.* presented an experimental and theoretical study that examined the mechanisms underlying the sorption process on carbon surfaces, characterizing two surface regions in which adsorption took place. In the low-coverage region, the heat of adsorption decreased rapidly for increased adsorbate concentrations, which was interpreted as a characteristic of a broad spectrum of binding sites.[200] At high loadings, the heat was found to be nearly independent of the extent of loading. Levesque and Lamari[201] calculated the isosteric heat of CO_2 adsorption on activated carbon using GCMC simulations. The authors discussed the possibility of estimating the isosteric heat of a macroscopic sample from adsorption isotherms computed for a distribution of slit pores of a given size.

Tenney and Lastoskie[202] performed GCMC simulations to investigate the influence of surface heterogeneity on the predicted adsorption behavior in activated carbons and coal. Isotherms were calculated for CO_2 adsorption inside slit-shaped pores characterized by several levels of chemical heterogeneity, such as oxygen and hydrogen content, pore width, and surface functional group orientation. The heterogeneities were present on the scale of $\sim$10 nm^2. The computed adsorption capacity was observed to increase in regions containing an excess of surface oxygen content, although exceptions to this trend were observed. Electrostatic adsorbate–adsorbent interactions significantly influenced adsorption on the model surfaces.

The preparation of mesoporous carbon materials with a narrow PSD and crystallographically organized pores has been described previously.[203] For a detailed review of the preparation of these materials and their related silica materials, the reader is referred to Zhao *et al.*[204] These preparations typically involved a multistep procedure in which a mesoporous silica mold was produced with the help of amphiphilic molecules. The mold was then filled with carbon-containing moieties that were subsequently carbonized. Finally, the silica mold was removed by chemical means. CO_2 adsorption on these ordered mesoporous carbons has been studied previously.[45] Peng *et al.*[205] carried out GCMC simulations to investigate the adsorption of CH_4 and CO_2 mixtures on the ordered carbon material CMK-1, to study the effects of temperature, pressure, pore width, and bulk composition on adsorption capacity, the local density profile, snapshots, and the solid–fluid potential curves. In this context, a snapshot means the spatial distribution of CO_2 and CH_4 at a certain moment in time. The electrical and thermal properties of carbon render it a good adsorbent for electrically induced temperature swing adsorption processes.

Liu *et al.*[206] developed an improved non-linear DFT (NLDFT) technique and combined this approach with PSD analysis of adsorbent activated carbon materials. They predicted the adsorption equilibria of high-pressure gas mixtures onto activated carbon. For two gas mixtures, CH_4/N_2 and CO_2/N_2, the authors improved the predictability of the adsorption equilibrium in the gas mixtures under high-pressure conditions, particularly the predictability of the weakly adsorbed species. CMC simulations were carried out by Cao and Wu[207] to investigate the separation of H_2 and CO_2 *via* adsorption in activated carbons using slit-pore models. At room temperature, the CO_2-over-H_2 selectivity reached approximately 90 : 1, indicating that H_2 and CO_2 could be efficiently separated. Heuchel *et al.*[208] predicted the adsorption properties of pure single-component gases and binary mixtures of CH_4 and CO_2 on a specific activated carbon, A35/4, using GCMC simulations. The PSD for the carbon was determined from the CH_4 and CO_2 isotherms at 293 K. Using the PSD and simulated adsorption densities in single pores, it was possible to predict, in good agreement with experiment data, (i) the adsorption ratios of binary mixtures containing CO_2 and CH_4, and (ii) the adsorption of both pure components at higher temperatures.

2.5.2 CMS. CMSs belong to a special class of activated carbons with molecule-sized narrow pores. They are typically

prepared by carbonization of coconut shell granules (or similar material), activation, and the subsequent deposition of an aromatic molecule by chemical vapor deposition (CVD), and carbonization of the aromatic molecule (benzene or similar). The resulting activated carbon molecular sieves have been commercialized for a variety of gas separation processes, and they have been applied in the production of ultrapure N_2. The purification of N_2 takes advantage of the differences in diffusion coefficients for N_2 and O_2 in certain CMSs.[4,23] For a detailed description of the kinetic enhancement of gas separation, see, for example, Ruthven and Reyes.[209]

The adsorption capacity and sorption kinetics of CO_2 and N_2 were studied by Vyas *et al.* on CMSs with varying amounts of deposited coke. Large amounts of deposited coke were correlated with a high capacity for CO_2 sorption.[210] Ahmad and coworkers studied CO_2 uptake by CMSs prepared from palm shells. The most suitable samples for CO_2-over-N_2 selection were those prepared at an intermediate carbonation temperature of 1273 K, with a deposition time longer than 20 min.[211–213] Carrot *et al.* prepared CMSs from polyester fibers and CVD of benzene at 1073 K, obtaining the best sorbents after 10 min of coke deposition. Still, these sorbents had a smaller capacity for CO_2 than the commercial CMS Takeda 3A sorbent.[214] CO_2 sorption on Takeda 3A was studied in detail by Rutherford *et al.*, who also studied CO_2 uptake in CMS-5A.[215–217] Yang *et al.* studied the kinetic separation of CH_4/CO_2 on CMSs,[65] and Nabais *et al.* prepared monolithic CMS materials by carbonization and activation, and observed excellent CO_2-over-N_2 selectivities.[218] Jayaraman *et al.* analyzed the utility of two commercial CMSs, Bergbau-Forschung and Takada 3A, in two process cycles, and focused on enhancing the separation by taking advantage of the differential diffusion rates of CO_2 and CH_4 in these commercial CMSs.[219] Campo *et al.*[220] studied transport mechanisms by comparing a CMS membrane with a commercial CMS adsorbent. The adsorption equilibrium isotherms of N_2, Ar, CO_2, and O_2 were determined.

Lafyatis *et al.* synthesized and studied the uptake of CO_2 in a series of CMSs. They derived CMSs from poly(furfuryl alcohol) and studied how the carbonization temperature and time affected the microporosity. High capacities were observed for the uptake of CO_2: nearly 8 wt% at a relative pressure of 0.015 (P/P_0). The diffusivity of CO_2 was shown to decrease for CMSs with smaller pores.[221] Solid-state nuclear magnetic resonance (^{13}C NMR) spectroscopy has been used to show the presence of furanic rings in samples pyrolyzed at relatively low temperatures. The presence of these moieties was correlated with CO_2 diffusivities in these materials.[222] Nguyen and Bhatia[223] studied the accessibility of Ar, N_2, CH_4, and CO_2 in disordered microporous carbons, using TST, MD simulations, and reverse Monte Carlo (RMC) simulations with realistic carbon models, in an effort to understand the kinetic restrictions imposed on adsorbate molecules by the narrow pore mouths of coals and molecular sieve carbons.

Fomkin[224] experimentally examined the CO_2 uptake in a range of adsorbents, including the microporous carbon AUK, at various temperatures and pressures. Pantatosaki *et al.*[225] used GCMC simulations and experimental adsorption isotherms to characterize microporous carbon and to obtain the PSD. They obtained PSDs under the assumption of slit and cylindrical pores at temperatures of 298 and 308 K. Steriotis *et al.*[226] and Samios *et al.*[227] used GCMC simulations to study the structural configurations of CO_2 molecules adsorbed in microporous carbons. The authors discussed the local density profiles and angular distributions of the axes of the adsorbed molecules within the pores. These calculations addressed the densification process and molecular packing in the micropores.

Samios *et al.*[228] used GCMC simulations and CO_2 experimental isotherm data at low and high temperatures to characterize the microporous carbon materials. They studied the PSD, the densification process in the micropores, and the structure of CO_2 molecular packing within the individual pores, addressing the effects on the local density of temperature, pore size, electric field gradient–electric quadrupole interactions, and molecular elongation of the adsorbates. Vishnyakov *et al.*[229] studied CO_2 adsorption in slit-shaped carbon micropores at 273 K using GCMC simulations and NLDFT. For pore widths in the range 0.3–1.5 nm, NLDFT estimations of the CO_2 adsorption isotherms were generally in agreement with the GCMC estimations. Samios *et al.*[230] developed a method to determine PSDs in the micropore regime, based on GCMC simulations and measured isotherms.

2.5.3 CNT. Carbon nanotubes (CNTs) have properties that promote CO_2 sorption. CNTs have been studied experimentally and theoretically with respect to CO_2 capture. In a combined theoretical and experimental study, Cinke *et al.* showed that single-walled CNTs (SWNTs) adsorbed twice the amount of CO_2 as did the corresponding activated carbon.[231] Zhao *et al.* studied the uptake of several gases, including CO_2, in SWNTs.[232] The authors deduced that adsorption proceeded mainly through physisorption. Anson *et al.* experimentally studied CO_2 adsorption, revealing a detailed picture of the structure and surfaces of certain SWNTs.[233] Infrared spectroscopy has indicated the presence of several types of CO_2 adsorption site in SWNTs, suggesting that CO_2 may become permanently trapped in SWNTs.[234,235] Su *et al.* argued, *via* an experimental study, that multi-walled CNTs (MWNTs) were good candidates for the low-temperature separation of CO_2 from flue gases.[236]

Ravikovitch *et al.*[237] presented a unified approach to pore size characterization in microporous carbonaceous materials, such as activated carbon and carbon fibers, using N_2, Ar, and CO_2 adsorption measurements based on NLDFT and GCMC methods. Huang *et al.*[238] performed GCMC simulations to investigate the adsorption behavior of an equimolar CO_2/CH_4 mixture in the presence of CNTs. The authors performed simulations to model the adsorption of the gas mixture onto five armchair CNTs [(6, 6), (7, 7), (8, 8), (9, 9), and (10, 10)],† with diameters varying from 0.678 to 1.356 nm, at seven temperatures (283, 293, 303, 313, 323, 333, and 343 K) and under seven pressures (1, 5, 10, 15, 20, 25, and 30 MPa), to characterize the effects of temperature, pressure, and pore size on the adsorption behavior. The authors found that CO_2 was preferentially adsorbed onto the CNT surfaces under all conditions investigated. For each type of CNT, the adsorption capacity for CO_2

† X, Y in (X, Y) describes how a graphene layer is wrapped into a single wall CNT. The integers X and Y describe the size of the CNT and the orientation of the atomic layer of carbon. Armchair: X = Y.

was estimated to be much higher than that of CH_4. CO_2 adsorption in CNTs appeared to increase dramatically with increasing CNT diameter. The selectivity of CNTs for CO_2 was no higher than that of activated carbons, zeolites, and MOFs reported in the literature.

Konstantakou *et al.*[239] performed GCMC simulations, in combination with experimental data, to characterize adsorption in microporous carbons (AX-21 in particular), with the goal of determining the optimal PSD for adsorption. Adsorption isotherms were calculated from the GCMC simulations for several pore widths up to 3.0 nm and for the adsorption of H_2 at 77 K. Quantum corrections were introduced by applying the Feynman–Hibbs effective potential. Skoulidas *et al.*[240] used atomistic MD simulations to examine the adsorption and transport diffusion of CO_2 and N_2 in SWNTs at room temperature as a function of nanotube diameter. The results were consistent with previous predictions that transport diffusivity of molecules inside carbon nanotubes is extremely rapid relative to transport in other porous materials. Sinnott *et al.*[241] carried out MD simulations to study molecular motion and the separation of molecular mixtures in carbon nanotube systems, for mixtures of CH_4, C_2H_6, n-C_4H_{10}, i-C_4H_{10}, and CO_2. Not surprisingly, they found that molecules (at 300 K) diffused from areas of high density to areas of low density throughout the nanotubes.

Xu *et al.*[242,243] performed non-equilibrium MD (NEMD) simulations of transport and separation characteristics of binary and ternary gas mixtures consisting of CO_2, CH_4, and H_2 through a carbon nanopore in the presence of an external chemical potential gradient. The authors addressed the effects of temperature, feed composition, and pore size on transport properties, investigating in detail the adsorption and separation characteristics. Müller[244] performed GCMC simulations on the adsorption of N_2, CO_2, and C_2F_6 (three quadrupolar molecules) inside SWCNTs and predicted a tilted ordering not previously reported, which was rationalized as resulting from a combination of steric effects and an anisotropic attraction pattern.

Su and Lua[245] determined the theoretical upper limit of the permeation rate of gases (with different masses, for activation energies of 0 kJ mol^{-1}) by the Knudsen diffusion mechanism. The distribution and magnitude of the potential energy of interaction between gas molecules and the carbon pore wall was strongly dependent on the pore size in the modeled membrane. MC simulations were performed by Jia *et al.*[246] to investigate the separation behavior of gas mixtures composed of CO_2 and N_2, using a model of a carbon membrane under various conditions. These calculations indicated that CO_2 was strongly adsorbed on the surface of the membrane. Yang and Zhong[247] carried out extensive GCMC simulations to study the adsorption behavior and orientational structure of CO_2 confined in slit graphite pores.

2.5.4 Nanobuds, graphenes. More "exotic" high-surface-area carbons facilitate CO_2-over-N_2 selection due to their elaborate structural and electronic properties. Ghosh *et al.* studied the uptake of H_2 and CO_2 on graphene, revealing an uptake of up to 35 wt% at a pressure of 101 kPa and temperature of 195 K.[68] Gauden and Wisniewski[248] carried out theoretical calculations to model the sorption of CO_2 on 4-ring graphene structures ("unmodified" or N-, O-, and OH-substituted) possessing a completely unsaturated edge-zigzag site. They reported results at the DFT B3LYP/6-31G(d,p) level of theory. Several theoretical reactivity indices, such as the ionization potential, electron affinity, global softness, and HOMO–LUMO gaps, were reported for the studied adsorbents. CO_2 was found to adsorb on the edge plane surface of N-, O-, and OH-containing carbon surfaces to a comparable or lesser degree to adsorption on the "unmodified" adsorbents.

With the goal of designing new carbon materials, Terzyk *et al.*[249] performed GCMC simulations to test the ability of fullerene-intercalated graphene nanocontainers (NanoBuds) to adsorb CH_4 and CO_2. By combining quantum mechanics and molecular simulations, Jiang and Sandler[28] investigated the adsorption of pure CO_2 and N_2, and their mixtures at room temperature in C168 schwarzite, as a model for nanoporous carbons. Schwarzites are theoretical bicontinuous porous structures analogous to fullerenes. The inclusion of the adsorbates' electric quadrupole moment in the simulation did not affect N_2 adsorption, although it did affect CO_2 adsorption at high coverage. The selective adsorption of CO_2 over N_2 by C-168 schwarzite, using a model flue gas, was predicted to be significantly higher when *ab initio* potentials were used than when the Steele potential was used, illustrating the importance of an accurate adsorbate–adsorbent interaction potential in determining gas adsorption. Nanohorns are small, open nanoscaled carbon objects. Urita *et al.* studied the semiconducting behavior of nanohorns under CO_2 and O_2 adsorption, reporting increased conductivity when CO_2 adsorbed to single-walled carbon nanohorns (SWNH), whereas the oxidized SWNH showed reduced conductivity upon CO_2 adsorption.[250] These findings may be relevant to electric swing adsorption.

2.6 Other porous oxides

γ-Alumina (γ-Al_2O_3) is commonly used as a porous support for a variety of catalytic applications. Dewaele *et al.* measured a high energy of desorption for CO_2 from a γ-alumina support with a surface area of 153 m^2 g^{-1}, as expected from the Lewis base character of the substrate.[251] Two commercial alumina substrates were studied by Rodrigues *et al.*, and one of the sorbents had a high capacity for CO_2 of 3.5 μmol m^{-2}.[252] Pokrovski *et al.* studied the adsorption of CO_2 on m-ZrO_2 (monoclinic) and t-ZrO_2 (tetragonal), and found a much higher CO_2 sorption capacity on m-ZrO_2 than on t-ZrO_2.[253] This observation was ascribed to the surface basicity of the monoclinic form. Knöfel *et al.* studied the uptake of CO_2 on mesoporous titania and found a high heat of CO_2 adsorption.[254]

Belmabkhout *et al.*[82,83] reported high equilibrium adsorption capacities and good separation capabilities for CO_2, CH_4, N_2, H_2, and O_2 in periodic mesoporous MCM-41 silica. MCM-41 is a hexagonally structured mesoporous material, and MCM-48 is a cubic structured mesoporous material in the class of M41S solids developed by Mobil in the late 1980s.[26] IAST was validated and used for the prediction of CO_2/N_2, CO_2/CH_4, and CO_2/H_2 binary mixture adsorption equilibria. MCM-41 showed preferential CO_2 adsorption over the other gases. Schumacher *et al.*[255] proposed a methodology with which to design hybrid organic–inorganic adsorbents, based on periodic mesoporous silicas using kMC simulations to generate realistic model adsorbents. The authors carried out GCMC simulations of adsorption in these

model materials. The capabilities of the method were demonstrated experimentally.

He and Seaton[256] reported the adsorption isotherms and the isosteric heats of adsorption of pure methane, ethane, and CO_2, and for mixtures of methane and CO_2, in the periodic mesoporous silica MCM-41. The energies of adsorption, for pure CO_2 and for CO_2 from a CO_2/methane mixture, were determined to be heterogeneously distributed, reflecting electrostatic interactions between CO_2 and the adsorbent. Yoshioka *et al.*[257] used NEMD simulations to study the mechanisms involved in pressure-driven gas permeation through a micropore on vitreous SiO_2 membranes. The study was performed to investigate the dependencies of the permeance of helium and CO_2 molecules on temperature and pore size. Yang *et al.*[258] carried out MD simulations of dense CO_2 on amorphous dehydroxylated silica surfaces. Permeability through molecular sieving membranes was investigated by Takaba *et al.*,[259] who employed GCMD to investigate the temperature dependence of H_2, Ne, Ar, O_2, N_2, and CO_2 adsorption. Activated transport was observed when the pore size of the membrane was smaller than 1.2 times the molecular diameter. Finally, Yoshioka *et al.*[260] used a particle-generating NEMD method to simulate He and CO_2 gas permeation at various temperatures and pressures through cylindrical pores that mimicked microporous silica.

2.7 Amine-modified mesoporous silica

Many studies have examined CO_2 adsorption in modified porous silica sorbents containing amine groups. The amine groups could be introduced by chemical surface modification or simply by coating or filling the pores. Previous studies have also investigated silica materials chemically modified by n-propylamine moieties.[72,75,261–268] Leal *et al.* showed that such amine-modified materials adsorbed significant amounts of CO_2 and that CO_2 was chemisorbed on the material.[261] Angeletti *et al.* showed that the same modifications produced excellent sites for Knoevenagel condensation.[268] Huang *et al.* studied CO_2 uptake under dry and moist conditions on MCM-48 modified with propylamine functional groups and found that the presence of water doubled the amount of CO_2 adsorbed.[75] Chaffee *et al.* observed a similar uptake from "wet CO_2", although the rate of uptake was lower than that under dry conditions.[263]

Sayari *et al.* expanded the pores of MCM-48 and modified them with pendant n-propylamine moieties. The authors concluded that the mechanisms describing the interaction between CO_2 and the amine functionalities were related to the chemistry present in amine solutions. Bicarbonate appeared to form only when large amounts of water were present; *i.e.* at conditions under which capillary condensation of water took place. Under dry conditions, propylammonium + propylcarbamate ion pairs formed.[266] Che *et al.* used a new chemistry to synthesize n-propylamine-functionalized silica materials (the AMS class[269]) in a highly controlled manner, although this chemistry does not introduce a large number of amine groups. Kim *et al.* studied the CO_2 uptake on such sorbents.[74]

Mesoporous silicas modified with amine or amine-like functionalities other than propylammonium have also been studied.[70,75–79,264,270] Kim *et al.* modified MCM-48 substrates with n-propylamine, polymeric n-propylamine, pyrrolidinepropyl, and polyethyleneimine (PEI) and observed that the highest capacity for CO_2 sorption was achieved by the n-propylamine-modified substrate.[264] Zelenak *et al.* showed that the n-aminopropyl-modified material had the highest capacity among three modifications studied: n-propylamine, 3-(methylamino)propyl, and 3-(phenylamino)propyl. A high basicity produced high levels of CO_2 sorption. Weak bases showed rapid regeneration, which may be beneficial in practical applications.[70] Zhao *et al.* showed that n-propylamine modifications yielded the highest capacities for CO_2 uptake among the modifications studied (n-propylamine, bis-ethanol amine, and amidine).[270] Ionic liquids tethered to silica and quaternary amines catalytically produced cyclic carbonates from adsorbed CO_2.[271]

Harlick and Sayari studied the performance of CO_2 adsorption on triamine-modified MCM-41.[75–78] The material, with expanded pores, showed significant advantages relative to the non-expanded material, and was found to outperform zeolite X in humid environments. Covalently tethered polyethyleneimine[272] on mesoporous silica has been shown to effectively capture CO_2 in a reversible manner.[72,273] The high amine loading, as well as the chemical anchoring of the alkaline moieties to the silica surface, made these materials highly useful for CO_2 capture.

Previous studies have examined CO_2 sorption in mesoporous silica, in which the pores have been physically filled with amines.[73,83,274–277] The CO_2-uptake capacities of these materials are large, but their tolerance for recycling processes, without leaching the filler material, remains under investigation.[74] Xu *et al.* studied the CO_2 uptake in MCM-41 materials filled with PEI and observed high capacities with an atypical temperature dependence. The materials adsorbed more CO_2 at higher temperatures than at low temperatures.[73,274–277] An uptake as high as 24.6 wt% CO_2/PEI was observed, which is higher than the uptake of pure PEI.[275] Chen *et al.* studied CO_2 absorption in monolithic silica with hierarchically textured pores impregnated with amines, for tetraethylenepentamine (TEPA) a high uptake was observed.[79]

CO_2 has been shown to chemisorb on many solids.[278–280] Chemisorption of CO_2 on porous silica materials, modified with n-propylamine, has been studied by infrared spectroscopy.[73,254,280–282] The chemistries of CO_2 and amines are well understood. Thermally unstable ammonium carbamate salts have been shown to form in the absence of water, releasing CO_2 upon heating.[283] Battjes *et al.* showed that alkylammonium–carbamate ion pairs were the product of a reaction between primary or secondary amines and CO_2.[284] At low temperatures (273 K), the dimeric form of carbamic acid was observed as the chemisorption product.[285,286] CO_2 was chemisorbed on n-propylamine-modified silica *via* two different mechanism in the presence or absence of water.[77,266,274,275,280,287,288] The carbamate ion pairs were shown to react with CO_2 and H_2O to form bicarbonate groups in the following ratios: one mole of amines chemisorbed one mole CO_2 in the presence of water; in the absence of water, two amines were required to chemisorb one mole of CO_2. One of the authors of this review recently detected both chemisorbed and physisorbed CO_2 on mesocaged silica adsorbents tethered by n-propylamines. Sorbents that were post-synthetically modified with n-propylamines took up more CO_2 at high temperatures than at low temperatures, indicating the

presence of a kinetic barrier. A high degree of heterogeneity in the coating was required to promote the formation of propylammonium-propylcarbamate ion pairs.[289]

The activation of sorbents using amine groups has attracted interest because it provides a method for achieving higher selectivity of CO_2 adsorption from flue gases. Gray *et al.* determined, somewhat surprisingly, that amine-enriched carbon sorbents had much lower capacities for CO_2 adsorption than did commercially available carbon sorbents.[290] Lu *et al.* prepared composite materials in which 3-aminopropyltriethoxysilane was condensed onto zeolites, activated carbons, and CNTs. The highest uptake was observed for the amine–CNT composite.[291] Dillon *et al.* covalently attached PEI to fluorinated SWNTs and studied adsorption on these materials using a variety of techniques. They found a high CO_2 uptake (9.2% w/w) and discussed various potential applications of the PEI-SWNTs composites.[292] One of the authors of this review has studied CO_2 uptake in porous carbons derived from hydrothermally treated glucose to which were attached chemically tethered amine functional groups; these materials showed a high level of CO_2 uptake.[84]

Only a few molecular simulation studies can be found for these systems. Chaffee[293] prepared a series of silica models with mesoporous dimensions, 3-D periodicity, varying pore diameter (22–33 Å), and with a varying density of silanol functional groups (2–9 OH per nm^2) on the internal surfaces. Models of inorganic–organic hybrid material were prepared by attaching grafted aminopropylhydroxysilyl groups at the locations providing the greatest (calculated) energy relief. The gas–solid molecular behavior at the modified interface were analyzed and visualized. Chen *et al.*[294] prepared an atomistic slit model to represent the propylamine-grafted mesoporous amorphous silica pore surface. Applying GCMC, they simulated CO_2, CO_2/N_2, CO_2/H_2O mixtures adsorption isotherms, studied the effects of temperature, calculated the selectivity of CO_2 over N_2. They predicted high CO_2/N_2 selectivity upon the amine modification of this amorphous silica material. In combination with calculations using quantum mechanics, the influence of H_2O on the CO_2 uptake were studied. The diffusion of CO_2 and H_2O was estimated by MD simulations.

2.8 Hydrotalcite and other sorbents

Many studies have investigated chemisorbents for CO_2, mainly Hydrotalcites (HTlc) and calcium oxide-based sorbents. For a detailed review, we refer the reader to Choi *et al.*[24] Here, we include some selected references to highlight the importance of these sorbents for the capture of CO_2 from point sources. HTlc was studied as a selective adsorbent for CO_2. HTlcs are alkaline clays (layered double hydroxides).[295–300] Yong *et al.* studied Pural™ MG50 and MG70 and showed CO_2 sorption (at 573 K and 100 kPa) exceeding 0.3 mmol g^{-1}.[295] Ritter *et al.* showed that potassium-exchanged HTlcs adsorbed CO_2 reversibly at high temperatures.[296–299] Yavuz *et al.* studied Ga^{3+}-substituted HTlc, which, together with K^+, proved to be a robust and promising material for sorption of CO_2.[300] Lee and Sircar proposed a temperature swing adsorption process using Na_2O on an alumina substrate,[301] and Wu *et al.* studied a calcium-based sorbent for CO_2 capture.[302] Notably, this sorbent had the potential for use in precombustion CO_2 capture. Solieman *et al.* studied Li_2ZrO_3, BaO, and CaO sorbents, with CaO found to be the most suitable sorbent for reforming methane.[303]

Dolomite is an inexpensive sedimentary $MgCaCO_3$ material and is a weak Lewis base. Duffy *et al.* studied the adsorption properties of dolomite towards acidic gases.[304] The surface area was increased in a process in which some MgO was produced, but the CO_2 capacity was not very high. Rajabbeigi *et al.*[305,306] developed models for nanoporous materials and inorganic membranes, in which interconnected pores of irregular shapes, sizes, and connectivity were used to model adsorption in three silicon carbide (carborundum) membranes. Non-equilibrium MD methods were used to study the transport and separation properties of this membrane in the presence of two binary gaseous mixtures, H_2/CO_2 and H_2/CH_4. Bulnes *et al.*[307] studied the adsorption of binary mixtures on solid heterogeneous substrates using MC simulation of a lattice gas model. The adsorption process was monitored *via* total and partial isotherms, and *via* the difference in heats of adsorption for the species in the mixture. The uptake of acidic gases by calcite ($CaCO_3$) was studied by Santschi and Rossi, who reported that CO_2 interacted specifically with calcite and formed bicarbonates with OH groups on the surface.[308] Mömming *et al.* studied the sorption of CO_2 using a frustrated Lewis acid–base pair composed of an organic borane and an organic phosphine.[309,310] A similar approach may potentially be used on porous substrates.

3. Conclusions

In this review, we attempted to provide an overview of the significant results related to CO_2 sorbent development, from the perspective of materials and theoretical chemistry. Such developments would benefit from collaborations between experimentalist and theoreticians. We hope that there will be more truly interdisciplinary studies on CO_2 sorbents, where chemical, physical, and engineering aspects are treated in an integrated manner.

We discussed the materials in eight groups: zeolites and microporous silicates, aluminium phosphates, MOFs, COFs, carbons, other porous oxides, amine-modified mesoporous silicas, hydrotalcite and other sorbents. In screening and designing of MOFs, better force fields are needed and searches for such are ongoing. Many of these sorbents show great potential as CO_2 sorbents. Amine-modified porous solids have been studied in detail experimentally, but only few theoretical studies of these complex solids have been performed. These amine-containing solids show high CO_2-over-N_2 selectivity, high operational efficiency, and are robust towards water. They could potentially be used; however, a fair amount of engineering studies need to be performed.

Additional developments in developing CO_2 sorbents are forthcoming, and we are certain that combined experimental and theoretical approaches will enable the development of CO_2-selective sorbents, without the energetic penalties associated with strong chemisorbents. Zeolites are typically hydrophilic and render them difficult to use for CO_2 capture from flue gases. Hydrophobic microporous solids are more robust towards the presence of water vapor. Many different sorbents (zeolites, CMS,

$ALPO_4$, silicates, MOFs, COFs) could potentially enable molecular sieving or kinetic selection of CO_2-over-N_2. In our opinion, only a few studies have seriously considered the prospects for developing kinetically active or molecular sieving as a means of separating CO_2 from N_2-rich flue gas.

References

1 S. Rackley, *Carbon Capture and Storage*, Butterworth-Heinemann, Cambridge, 2009.
2 D. Aaron and C. Tsouris, *Sep. Sci. Technol.*, 2005, **40**, 321–348.
3 R. M. A. Roque-Malherbe, *Adsorption and Diffusion in Nanoporous Materials*, CRC Press, Baton Rouge, 2007.
4 R. T. Yang, *Gas Separation by Adsorption Processes*, Imperical College Press, London, 1997.
5 J. Baxter, Z. Bian, G. Chen, D. Danielson, M. S. Dresselhaus, A. G. Fedorov, T. S. Fisher, C. W. Jones, E. Maginn, U. Kortshagen, A. Manthiram, A. Nozik, D. R. Rolison, T. Sands, L. Shi, D. Sholl and Y. Wu, *Energy Environ. Sci.*, 2009, **2**, 559–588.
6 M. T. Ho, G. W. Allinson and D. E. Wiley, *Ind. Eng. Chem. Res.*, 2008, **47**, 4883–4890.
7 D. M. Ruthven, *Principles of Adsorption and Adsorption Processes*, John Wiley & Sons, Inc., New York, 1984.
8 J. A. Dunne, M. Rao, S. Sircar, R. J. Gorte and A. L. Myers, *Langmuir*, 1996, **12**, 5896–5904.
9 P. J. E. Harlick and F. H. Tezel, *Microporous Mesoporous Mater.*, 2004, **76**, 71–79.
10 D. W. Breck, W. G. Eversole, R. M. Milton, T. B. Reed and T. L. Thomas, *J. Am. Chem. Soc.*, 1956, **78**, 5963–5971.
11 A. R. Millward and O. M. Yaghi, *J. Am. Chem. Soc.*, 2005, **127**, 17998–17999.
12 P. L. Llewellyn, S. Bourrelly, C. Serre, A. Vimont, M. Daturi, L. Hamon, G. De Weireld, J. Chang, D. Hong, Y. K. Hwang, S. H. Jhung and G. Ferey, *Langmuir*, 2008, **24**, 7245–7250.
13 H. Furukawa and O. M. Yaghi, *J. Am. Chem. Soc.*, 2009, **131**, 8875–8883.
14 S. Sircar, T. C. Golden and M. B. Rao, *Carbon*, 1996, **34**, 1–12.
15 D. Frenkel and B. Smit, *Understanding of Molecular Simulation: From Algorithms to Applications*, Academic Press, San Diego, 2002.
16 D. Nicholson and N. G. Parsonage, *Computer Simulation and the Statistical Mechanics of Adsorption*, Academic Press, San Diego, 1982.
17 T. Watanabe, S. Keskin, S. Nair and D. S. Sholl, *Phys. Chem. Chem. Phys.*, 2009, **11**, 11389–11394.
18 A. García-Sánchez, C. O. Ania, J. B. Parra, D. Dubbeldam, T. J. H. Vlugt, R. Krishna and S. Calero, *J. Phys. Chem. C*, 2009, **113**, 8814–8820.
19 Z. Yong, V. Mata and A. E. Rodrigues, *Sep. Purif. Technol.*, 2002, **26**, 195–205.
20 K. B. Lee, M. G. Beaver, H. S. Caram and S. Sircar, *Ind. Eng. Chem. Res.*, 2008, **47**, 8048–8062.
21 C. M. White, B. R. Strazisar, E. J. Granite, J. S. Hoffman and H. W. Pennline, *J. Air Waste Manage. Assoc.*, 2003, **53**, 645–715.
22 D. M. Ruthven, F. Shamsuzzaman and K. S. Knaebel, *Pressure Swing Adsorption*, John Wiley and Sons, Inc, New York, 1994.
23 S. Choi, J. H. Drese and C. W. Jones, *ChemSusChem*, 2009, **2**, 796–854.
24 D. W. Breck, *Zeolite Molecular Sieves*, Robert E. Krieger Pub. Co., Malabar, 1984.
25 R. C. Reid, J. M. Prausnitz and T. K. Sherwood, *The Properties of Gases and Liquids*, McGraw-Hill, New York, 1977.
26 J. S. Beck, J. C. Vartuli, W. J. Roth, M. E. Leonowicz, C. T. Kresge, K. D. Schmitt, C. T. W. Chu, D. H. Olson, E. W. Sheppard, S. B. Mccullen, J. B. Higgins and J. L. Schlenker, *J. Am. Chem. Soc.*, 1992, **114**, 10834–10843.
27 D. Y. Zhao, J. L. Feng, Q. S. Huo, N. Melosh, G. H. Fredrickson, B. F. Chmelka and G. D. Stucky, *Science*, 1998, **279**, 548–552.
28 J. W. Jiang and S. I. Sandler, *J. Am. Chem. Soc.*, 2005, **127**, 11989–11997.
29 B. Liu and B. Smit, *Langmuir*, 2009, **25**, 5918–5926.
30 A. K. Rappe, C. J. Casewit, K. S. Colwell, W. A. Goddard and W. M. Skiff, *J. Am. Chem. Soc.*, 1992, **114**, 10024–10051.
31 S. L. Mayo, B. D. Olafson and W. A. Goddard, *J. Phys. Chem.*, 1990, **94**, 8897–8909.
32 S. Keskin, J. C. Liu, J. K. Johnson and D. S. Sholl, *Microporous Mesoporous Mater.*, 2009, **125**, 101–106.
33 K. S. Walton, A. R. Millward, D. Dubbeldam, H. Frost, J. J. Low, O. M. Yaghi and R. Q. Snurr, *J. Am. Chem. Soc.*, 2008, **130**, 406–407.
34 A. Ö. Yazaydin, R. Q. Snurr, T.-H. Park, K. Koh, J. Liu, M. D. LeVan, A. I. Benin, P. Jakubczak, M. Lanuza, D. B. Galloway, J. J. Low and R. R. Willis, *J. Am. Chem. Soc.*, 2009, **131**, 18198–18199.
35 F. Salles, A. Ghoufi, G. Maurin, R. G. Bell, C. Mellot-Draznieks and G. Férey, *Angew. Chem., Int. Ed.*, 2008, **47**, 8487–8491.
36 F. Salles, H. Jobic, A. Ghoufi, P. L. Llewellyn, C. Serre, S. Bourrelly, G. Férey and G. Maurin, *Angew. Chem., Int. Ed.*, 2009, **48**, 8335–8339.
37 P. Dauber-Osguthorpe, V. A. Roberts, D. J. Dauber-Osguthorpe, J. Wolf, M. Genest and A. T. Hagler, *Proteins: Struct., Funct., Genet.*, 1988, **4**, 31–47.
38 F. L. Hirshfeld, *Theor. Chim. Acta*, 1977, **44**, 129.
39 R. S. Mulliken, *J. Chem. Phys.*, 1955, **23**, 1833–1840.
40 C. M. Breneman and K. B. Wiberg, *J. Comput. Chem.*, 1990, **11**, 361–373.
41 H. Besler, K. M. Merz and P. A. Kollman, *J. Comput. Chem.*, 1990, **11**, 431–439.
42 N. A. Ramsahye, G. Maurin, S. Bourrelly, P. L. Llewellyn, T. Loiseau and G. Ferey, *Phys. Chem. Chem. Phys.*, 2007, **9**, 1059–1063.
43 N. L. Allinger, Y. H. Yuh and J.-H. Lii, *J. Am. Chem. Soc.*, 1989, **111**, 8551–8566.
44 M. Tafipolsky and R. Schmid, *J. Phys. Chem. B*, 2009, **113**, 1341–1352.
45 N. A. Ramsahye, G. Maurin, S. Bourrelly, P. L. Llewellyn, T. Devic, C. Serre, T. Loiseau and G. Ferey, *Adsorption*, 2007, **13**, 461–467.
46 N. A. Ramsahye, G. Maurin, S. Bourrelly, P. L. Llewellyn, T. Loiseau, C. Serre and G. Férey, *Chem. Commun.*, 2007, 3261–3263.
47 J. G. Harris and K. H. Yung, *J. Phys. Chem.*, 1995, **99**, 12021–12024.
48 G. Maurin, P. L. Llewellyn and R. G. Bell, *J. Phys. Chem. B*, 2005, **109**, 16084–16091.
49 J. J. Potoff and J. I. Siepmann, *AlChE J.*, 2001, **47**, 1676–1682.
50 M. G. Martin and J. I. Siepmann, *J. Phys. Chem. B*, 1998, **102**, 2569–2577.
51 C. S. Murthy, K. Sing, M. L. Klein and I. R. McDonald, *Mol. Phys.*, 1980, **41**, 1387–1399.
52 S. Y. Jiang, K. E. Gubbins and J. A. Zollweg, *Mol. Phys.*, 1993, **80**, 103–116.
53 X. Xu, X. Zhao, L. Sun and X. Liu, *J. Nat. Gas Chem.*, 2009, **18**, 167–172.
54 J. A. Delgado, M. A. Uguina, J. M. Gómez and L. Ortega, *Sep. Purif. Technol.*, 2006, **48**, 223–228.
55 K. A. Fisher, K. D. Huddersman and M. J. Taylor, *Chem.–Eur. J.*, 2003, **9**, 5873–5878.
56 A. Zukal, I. Dominguez, J. Mayerová and J. Čejka, *Langmuir*, 2009, **25**, 10314–10321.
57 C. Martin, N. Tosi-Pellenq, J. Patarin and J. P. Coulomb, *Langmuir*, 1998, **14**, 1774–1778.
58 X. X. Zhao, X. L. Xu, L. B. Sun, L. L. Zhang and X. Q. Liu, *Energy Fuels*, 2009, **23**, 1534–1538.
59 M. E. Rivera-Ramos, G. J. Ruiz-Mercado and A. J. Hernandez-Maldonado, *Ind. Eng. Chem. Res.*, 2008, **47**, 5602–5610.
60 I. Deroche, L. Gaberova, G. Maurin, P. L. Llewellyn, M. Castro and P. A. Wright, *Adsorption*, 2008, **14**, 207–213.
61 H. Hayashi, A. P. Cote, H. Furukawa, M. O'Keeffe and O. M. Yaghi, *Nat. Mater.*, 2007, **6**, 501–506.
62 B. Wang, A. P. Cote, H. Furukawa, M. O'Keeffe and O. M. Yaghi, *Nature*, 2008, **453**, 207–U6.
63 S. Bourrelly, P. L. Llewellyn, C. Serre, F. Millange, T. Loiseau and G. Férey, *J. Am. Chem. Soc.*, 2005, **127**, 13519–13521.
64 F. Debatin, A. Thomas, A. Kelling, N. Hedin, Z. Bacsik, I. Senkovska, S. Kaskel, M. Junginger, H. Müller, U. Schilde, C. Jäger, A. Friedrich and H.-J. H, *Angew. Chem., Int. Ed.*, 2010, **49**, 1258–1262.
65 A. Kapoor and R. T. Yang, *Chem. Eng. Sci.*, 1989, **44**, 1723–1733.

66 T. D. Burchell, R. R. Judkins, M. R. Rogers and A. M. Williams, *Carbon*, 1997, **35**, 1279–1294.
67 T. C. Drage, J. M. Blackman, C. Pevida and C. E. Snape, *Energy Fuels*, 2009, **23**, 2790–2796.
68 A. Ghosh, K. S. Subrahmanyam, K. S. Krishna, S. Datta, A. Govindaraj, S. K. Pati and C. N. R. Rao, *J. Phys. Chem. C*, 2008, **112**, 15704–15707.
69 G. Chandrasekar, W. J. Son and W. S. Ahn, *J. Porous Mater.*, 2009, **16**, 545–551.
70 V. Zelenak, D. Halamova, L. Gaberova, E. Bloch and P. L. Llewellyn, *Microporous Mesoporous Mater.*, 2008, **116**, 358–364.
71 X. C. Xu, C. S. Song, J. M. Andresen, B. G. Miller and A. W. Scaroni, *Energy Fuels*, 2002, **16**, 1463–1469.
72 J. C. Hicks, J. H. Drese, D. J. Fauth, M. L. Gray, G. Qi and C. W. Jones, *J. Am. Chem. Soc.*, 2008, **130**, 2902–2903.
73 H. Y. Huang, R. T. Yang, D. Chinn and C. L. Munson, *Ind. Eng. Chem. Res.*, 2003, **42**, 2427–2433.
74 S. N. Kim, W. J. Son, J. S. Choi and W. S. Ahn, *Microporous Mesoporous Mater.*, 2008, **115**, 497–503.
75 P. J. E. Harlick and A. Sayari, *Ind. Eng. Chem. Res.*, 2007, **46**, 446–458.
76 P. J. E. Harlick and A. Sayari, *Ind. Eng. Chem. Res.*, 2006, **45**, 3248–3255.
77 R. S. Franchi, P. J. E. Harlick and A. Sayari, *Ind. Eng. Chem. Res.*, 2005, **44**, 8007–8013.
78 R. Franchi, P. J. E. Harlick and A. Sayari, *Stud. Surf. Sci. Catal.*, 2005, **156**, 879–886.
79 C. Chen, S. T. Yang, W. S. Ahn and R. Ryoo, *Chem. Commun.*, 2009, 3627–3629.
80 A. D. Ebner, S. P. Reynolds and J. A. Ritter, *Ind. Eng. Chem. Res.*, 2006, **45**, 6387–6392.
81 M. L. Gray, J. S. Hoffman, D. C. Hreha, D. J. Fauth, S. W. Hedges, K. J. Champagne and H. W. Pennline, *Energy Fuels*, 2009, **23**, 4840–4844.
82 Y. Belmabkhout and A. Sayari, *Chem. Eng. Sci.*, 2009, **64**, 3729–3735.
83 Y. Belmabkhout, R. Serna-Guerrero and A. Sayari, *Chem. Eng. Sci.*, 2009, **64**, 3721–3728.
84 L. Zhao, Z. Bacsik, N. Hedin, W. Wei, Y. H. Sun, M. Antonietti and M. M. Titirici, *ChemSusChem*, 2010, **3**, 840–845.
85 C. Baerlocher and L. B. McCusker, *Database of Zeolite Structures*, http://www.iza-structure.org/databases/.
86 R. M. Milton, US patent: 2 882 244, 1959.
87 R. M. Barrer and R. M. Gibbons, *Trans. Faraday Soc.*, 1965, **61**, 948.
88 S. Cavenati, C. A. Grande and A. E. Rodrigues, *J. Chem. Eng. Data*, 2004, **49**, 1095–1101.
89 F. Brandani and D. M. Ruthven, *Ind. Eng. Chem. Res.*, 2004, **43**, 8339–8344.
90 G. K. Papadopoulos and D. N. Theodorou, *Mol. Simul.*, 2009, **35**, 79–89.
91 Y. Nakazaki, Y. Tanaka, N. Goto and T. Inui, *Catal. Today*, 1995, **23**, 391–396.
92 W. Jia and S. Murad, *J. Chem. Phys.*, 2004, **120**, 4877–4885.
93 W. Jia and S. Murad, *J. Chem. Phys.*, 2005, **122**, 234708.
94 P. Galhotra, J. G. Navea, S. C. Larsen and V. H. Grassian, *Energy Environ. Sci.*, 2009, **2**, 401–409.
95 P. J. E. Harlick and F. H. Tezel, *Sep. Sci. Technol.*, 2005, **40**, 2569–2591.
96 W. Shao, L. Z. Zhang, L. X. Li and R. L. Lee, *Adsorption*, 2009, **15**, 497–505.
97 G. Maurin, Y. Belmabkhout, G. Pirngruber, L. Gaberova and P. L. Llewellyn, *Adsorption*, 2007, **13**, 453–460.
98 G. Maurin, R. Bell, B. Kuchta, T. Poyet and P. L. Llewellyn, *Adsorption*, 2005, **11**, 331–336.
99 A. Ghoufi, L. Gaberova, J. Rouquerol, D. Vincent, P. L. Llewellyn and G. Maurin, *Microporous Mesoporous Mater.*, 2009, **119**, 117–128.
100 D. F. Plant, G. Maurin, I. Deroche and P. L. Llewellyn, *Microporous Mesoporous Mater.*, 2007, **99**, 70–78.
101 D. F. Plant, G. Maurin, H. Jobic and P. L. Llewellyn, *J. Phys. Chem. B*, 2006, **110**, 14372–14378.
102 D. F. Plant, H. Jobic, P. L. Llewellyn and G. Maurin, *Adsorption*, 2007, **13**, 209–214.
103 A. Pulido, M. R. Delgado, O. Bludský, M. Rubeš, P. Nachtigall and C. O. Areán, *Energy Environ. Sci.*, 2009, **2**, 1187–1195.
104 D. F. Plant, G. Maurin, I. Deroche, L. Gaberova and P. L. Llewellyn, *Chem. Phys. Lett.*, 2006, **426**, 387–392.
105 A. Chatterjee and T. Iwasaki, *J. Phys. Chem. A*, 1999, **103**, 9857–9863.
106 K. Kusakabe, T. Kuroda, A. Murata and S. Morooka, *Ind. Eng. Chem. Res.*, 1997, **36**, 649–655.
107 S. S. Liu and X. N. Yang, *J. Chem. Phys.*, 2006, **124**, 244705.
108 E. Jaramillo and M. Chandross, *J. Phys. Chem. B*, 2004, **108**, 20155–20159.
109 E. D. Akten, R. Siriwardane and D. S. Sholl, *Energy Fuels*, 2003, **17**, 977–983.
110 J. Izumi, A. Yasutake, N. Tomonaga, N. Oka, H. Ota, N. Akutsu, S. Umeda and M. Tajima, *Stud. Surf. Sci. Catal.*, 1997, **105**, 2315–2322.
111 Q. L. Liu, A. Mace, Z. Bacsik, J. L. Sun, A. Laaksonen and N. Hedin, *Chem. Commun.*, 2010, **46**, 4502–4504.
112 E. M. Flanigen, J. M. Bennett, R. W. Grose, J. P. Cohen, R. L. Patton, R. M. Kirchner and J. V. Smith, *Nature*, 1978, **271**, 512–516.
113 J. A. Dunne, R. Mariwals, M. Rao, S. Sircar, R. J. Gorte and A. L. Myers, *Langmuir*, 1996, **12**, 5888–5895.
114 P. J. E. Harlick and F. H. Tezel, *Sep. Sci. Technol.*, 2002, **37**, 33–60.
115 P. J. E. Harlick and F. H. Tezel, *Sep. Purif. Technol.*, 2003, **33**, 199–210.
116 A. Hirotani, K. Mizukami, R. Miura, H. Takaba, T. Miya, A. Fahmi, A. Stirling, M. Kubo and A. Miyamoto, *Appl. Surf. Sci.*, 1997, **120**, 81–84.
117 T. Yamazaki, M. Katoh, S. Ozawa and Y. Ogino, *Mol. Phys.*, 1993, **80**, 313–324.
118 L. C. Geiger, B. M. Ladanyi and M. E. Chapin, *J. Chem. Phys.*, 1990, **93**, 4533–4542.
119 A. Zukal, J. Pawlesa and J. Čejka, *Adsorption*, 2009, **15**, 264–270.
120 J. M. Leyssale, G. K. Papadopoulos and D. N. Theodorou, *J. Phys. Chem. B*, 2006, **110**, 22742–22753.
121 X. P. Yue and X. N. Yang, *Langmuir*, 2006, **22**, 3138–3147.
122 G. K. Papadopoulos, H. Jobic and D. N. Theodorou, *J. Phys. Chem. B*, 2004, **108**, 12748–12756.
123 S. Himeno, M. Takenaka and S. Shimura, *Mol. Simul.*, 2008, **34**, 1329–1336.
124 E. García-Pérez, J. B. Parra, C. O. Ania, A. García-Sánchez, J. M. Van Baten, R. Krishna, D. Dubbeldam and S. Calero, *Adsorption*, 2007, **13**, 469–476.
125 S. E. Jee and D. S. Sholl, *J. Am. Chem. Soc.*, 2009, **131**, 7896–7904.
126 N. Hedin, G. J. DeMartin, W. J. Roth, K. G. Strohmaier and S. C. Reyes, *Microporous Mesoporous Mater.*, 2008, **109**, 327–334.
127 R. R. Chance, *229 ACS Nat M San Di* 2005.
128 R. Krishna and J. M. van Baten, *Chem. Eng. J.*, 2007, **133**, 121–131.
129 D. Selassie, D. Davis, J. Dahlin, E. Feise, G. Haman, D. S. Sholl and D. Kohen, *J. Phys. Chem. C*, 2008, **112**, 16521–16531.
130 R. Krishna and J. M. van Baten, *Sep. Purif. Technol.*, 2008, **61**, 414–423.
131 R. Krishna and J. M. van Baten, *Chem. Phys. Lett.*, 2007, **446**, 344–349.
132 R. Krishna, J. M. Van Baten, E. García-Pérez and S. Calero, *Ind. Eng. Chem. Res.*, 2007, **46**, 2974–2986.
133 R. Krishna, J. M. van Baten, E. García-Pérez and S. Calero, *Chem. Phys. Lett.*, 2006, **429**, 219–224.
134 J. Van Den Bergh, S. A. Ban, T. J. H. Vlugt and F. Kapteijn, *J. Phys. Chem. C*, 2009, **113**, 17840–17850.
135 R. Krishna and J. M. van Baten, *Chem. Eng. Sci.*, 2008, **63**, 3120–3140.
136 Y. Ohta, H. Takaba and S. I. Nakao, *Microporous Mesoporous Mater.*, 2007, **101**, 319–323.
137 A. Goj, D. S. Sholl, E. D. Akten and D. Kohen, *J. Phys. Chem. B*, 2002, **106**, 8367–8375.
138 J. R. Kiovsky and P. B. Koradia, US patent: 4 059 543, 1977.
139 G. Aguilar-Armenta, M. E. Patino-Iglesias and R. Leyva-Ramos, *Adsorpt. Sci. Technol.*, 2003, **21**, 81–91.
140 R. V. Siriwardane, M. S. Shen and E. P. Fisher, *Energy Fuels*, 2003, **17**, 571–576.
141 S. T. Wilson, B. M. Lok, C. A. Messina, T. R. Cannan and E. M. Flanigen, *J. Am. Chem. Soc.*, 1982, **104**, 1146–1147.

142 B. M. Lok, C. A. Messina, R. L. Patton, R. T. Gajek, T. R. Cannan and E. M. Flanigen, *J. Am. Chem. Soc.*, 1984, **106**, 6092–6093.
143 X. X. Guan, F. X. Zhang, G. J. Wu and N. J. Guan, *Mater. Lett.*, 2006, **60**, 3141–3144.
144 O. M. Yaghi, M. O'Keeffe, N. W. Ockwig, H. K. Chae, M. Eddaoudi and J. Kim, *Nature*, 2003, **423**, 705–714.
145 G. Férey, *Chem. Soc. Rev.*, 2008, **37**, 191–214.
146 J.-R. Li, R. J. Kuppler and H.-C. Zhou, *Chem. Soc. Rev.*, 2009, **38**, 1477–1504.
147 S. Keskin, J. Liu, R. B. Rankin, J. K. Johnson and D. S. Sholl, *Ind. Eng. Chem. Res.*, 2009, **48**, 2355–2371.
148 M. Tafipolsky, S. Amirjalayer and R. Schmid, *Microporous Mesoporous Mater.*, 2010, **129**, 304–318.
149 T. Düren, Y. S. Bae and R. Q. Snurr, *Chem. Soc. Rev.*, 2009, **38**, 1237–1247.
150 M. Eddaoudi, J. Kim, N. Rosi, D. Vodak, J. Wachter, M. O'Keeffe and O. M. Yaghi, *Science*, 2002, **295**, 469–472.
151 A. C. Sudik, A. R. Millward, N. W. Ockwig, A. P. Cote, J. Kim and O. M. Yaghi, *J. Am. Chem. Soc.*, 2005, **127**, 7110–7118.
152 R. Banerjee, A. Phan, B. Wang, C. Knobler, H. Furukawa, M. O'Keeffe and O. M. Yaghi, *Science*, 2008, **319**, 939–943.
153 Z. X. Zhao, Z. Li and Y. S. Lin, *Ind. Eng. Chem. Res.*, 2009, **48**, 10015–10020.
154 Q. Y. Yang, Q. Xu, B. Liu, C. L. Zhong and S. Berend, *Chin. J. Chem. Eng.*, 2009, **17**, 781–790.
155 B. Liu, Q. Y. Yang, C. Y. Xue, C. L. Zhong, B. Chen and B. Smit, *J. Phys. Chem. C*, 2008, **112**, 9854–9860.
156 L. Bastin, P. S. Bárcia, E. J. Hurtado, J. A. C. Silva, A. E. Rodrigues and B. Chen, *J. Phys. Chem. C*, 2008, **112**, 1575–1581.
157 P. S. Barcia, L. Bastin, E. J. Hurtado, J. A. C. Silva, A. E. Rodrigues and B. L. Chen, *Sep. Sci. Technol.*, 2008, **43**, 3494–3521.
158 P. S. Bárcia, J. A. C. Silva and A. E. Rodrigues, *AIChE J.*, 2007, **53**, 1970–1981.
159 P. S. Bárcia, J. A. C. Silva and A. E. Rodrigues, *Ind. Eng. Chem. Res.*, 2006, **45**, 4316–4328.
160 D. H. Liu, C. C. Zheng, Q. Y. Yang and C. L. Zhong, *J. Phys. Chem. C*, 2009, **113**, 5004–5009.
161 R. B. Rankin, J. C. Liu, A. D. Kulkarni and J. K. Johnson, *J. Phys. Chem. C*, 2009, **113**, 16906–16914.
162 R. Babarao and J. W. Jiang, *J. Am. Chem. Soc.*, 2009, **131**, 11417–11425.
163 R. Babarao and J. W. Jiang, *Energy Environ. Sci.*, 2009, **2**, 1088–1093.
164 N. A. Ramsahye, G. Maurin, S. Bourrelly, P. L. Llewellyn, C. Serre, T. Loiseau, T. Devic and G. Férey, *J. Phys. Chem. C*, 2008, **112**, 514–520.
165 C. Serre, S. Bourrelly, A. Vimont, N. A. Ramsahye, G. Maurin, P. L. Llewellyn, M. Daturi, Y. Filinchuk, O. Leynaud, P. Barnes and G. Férey, *Adv. Mater.*, 2007, **19**, 2246–2251.
166 D. S. Coombes, F. Corà, C. Mellot-Draznieks and R. G. Bell, *J. Phys. Chem. C*, 2009, **113**, 544–552.
167 L. Hamon, P. L. Llewellyn, T. Devic, A. Ghoufi, G. Clet, V. Guillerm, G. D. Pirngruber, G. Maurin, C. Serre, G. Driver, W. Van Beek, E. Jolimaître, A. Vimont, M. Daturi and G. Férey, *J. Am. Chem. Soc.*, 2009, **131**, 17490–17499.
168 A. Ö. Yazaydin, A. I. Benin, S. A. Faheem, P. Jakubczak, J. J. Low, Richard R. Willis and R. Q. Snurr, *Chem. Mater.*, 2009, **21**, 1425–1430.
169 Q. Y. Yang, C. Y. Xue, C. L. Zhong and J. F. Chen, *AIChE J.*, 2007, **53**, 2832–2840.
170 Z. J. Liang, M. Marshall and A. L. Chaffee, *Energy Fuels*, 2009, **23**, 2785–2789.
171 Y. Cheng, A. Rondo, H. Noguchi, H. Kajiro, K. Urita, T. Ohba, K. Kaneko and H. Kanoh, *Langmuir*, 2009, **25**, 4510–4513.
172 S. R. Miller, P. A. Wright, T. Devic, C. Serre, G. Ferey, P. L. Llewellyn, R. Denoyel, L. Gaberova and Y. Filinchuk, *Langmuir*, 2009, **25**, 3618–3626.
173 R. Babarao, Z. Q. Hu, J. W. Jiang, S. Chempath and S. I. Sandler, *Langmuir*, 2007, **23**, 659–666.
174 R. Babarao and J. W. Jiang, *Langmuir*, 2008, **24**, 5474–5484.
175 R. Babarao, J. W. Jiang and S. I. Sandler, *Langmuir*, 2009, **25**, 5239–5247.
176 R. Babarao, J. W. Jiang and S. I. Sandler, *Langmuir*, 2009, **25**, 6590.
177 D. Farrusseng, C. Daniel, C. Gaudillère, U. Ravon, Y. Schuurman, C. Mirodatos, D. Dubbeldam, H. Frost and R. Q. Snurr, *Langmuir*, 2009, **25**, 7383–7388.
178 A. Martín-Calvo, E. García-Pérez, J. Manuel Castillo and S. Calero, *Phys. Chem. Chem. Phys.*, 2008, **10**, 7085–7091.
179 Q. Y. Yang, C. L. Zhong and J. F. Chen, *J. Phys. Chem. C*, 2008, **112**, 1562–1569.
180 S. Keskin and D. S. Sholl, *Langmuir*, 2009, **25**, 11786–11795.
181 A. Demessence, D. M. D'Alessandro, M. L. Foo and J. R. Long, *J. Am. Chem. Soc.*, 2009, **131**, 8784.
182 Y. S. Bae, O. K. Farha, J. T. Hupp and R. Q. Snurr, *J. Mater. Chem.*, 2009, **19**, 2131–2134.
183 Z. Q. Wang and S. M. Cohen, *J. Am. Chem. Soc.*, 2009, **131**, 16675–16677.
184 Y. S. Bae, K. L. Mulfort, H. Frost, P. Ryan, S. Punnathanam, L. J. Broadbelt, J. T. Hupp and R. Q. Snurr, *Langmuir*, 2008, **24**, 8592–8598.
185 A. Torrisi, C. Mellot-Draznieks and R. G. Bell, *J. Chem. Phys.*, 2009, **130**, 194703.
186 A. Torrisi, C. Mellot-Draznieks and R. G. Bell, *J. Chem. Phys.*, 2010, **132**, 044705.
187 H. S. Choi and M. P. Suh, *Angew. Chem., Int. Ed.*, 2009, **48**, 6865–6869.
188 S. Satyapal, T. Filburn, J. Trela and J. Strange, *Energy Fuels*, 2001, **15**, 250–255.
189 P. M. Budd, B. S. Ghanem, S. Makhseed, N. B. McKeown, K. J. Msayib and C. E. Tattershall, *Chem. Commun.*, 2004, 230–231.
190 N. Ritter, M. Antonietti, A. Thomas, I. Senkovska, S. Kaskel and J. Weber, *Macromolecules*, 2009, **42**, 8017–8020.
191 R. Babarao and J. W. Jiang, *Energy Environ. Sci.*, 2008, **1**, 139–143.
192 Q. Y. Yang and C. L. Zhong, *Langmuir*, 2009, **25**, 2302–2308.
193 R. Babarao and J. W. Jiang, *Langmuir*, 2008, **24**, 6270–6278.
194 L. B. Adams, C. R. Hall, R. J. Holmes and R. A. Newton, *Carbon*, 1988, **26**, 451–459.
195 P. L. Walker, R. J. Foresti and C. C. Wright, *Ind. Eng. Chem.*, 1953, **45**, 1703–1710.
196 P. L. Walker Jr. and M. Shelef, *Carbon*, 1967, **5**, 7–11.
197 F. Brandani, A. Rouse, S. Brandani and D. M. Ruthven, *Adsorption*, 2004, **10**, 99–109.
198 S. Urbonaite, J. M. Juarez-Galan, J. Leis, F. Rodriguez-Reinoso and G. Svensson, *Microporous Mesoporous Mater.*, 2008, **113**, 14–21.
199 R. V. Siriwardane, M. S. Shen, E. P. Fisher and J. A. Poston, *Energy Fuels*, 2001, **15**, 279–284.
200 A. Montoya, F. Mondragón and T. N. Truong, *Carbon*, 2003, **41**, 29–39.
201 D. Levesque and F. D. Lamari, *Mol. Phys.*, 2009, **107**, 591–597.
202 C. M. Tenney and C. M. Lastoskie, *Environ. Prog.*, 2006, **25**, 343–354.
203 S. H. Joo, S. Jun and R. Ryoo, *Microporous Mesoporous Mater.*, 2001, **44–45**, 153–158.
204 Y. Wan and D. Y. Zhao, *Chem. Rev.*, 2007, **107**, 2821–2860.
205 X. Peng, D. P. Cao and J. S. Zhao, *Sep. Purif. Technol.*, 2009, **68**, 50–60.
206 S. Liu, X. Yang and Z. Yang, *Chin. Sci. Bull.*, 2008, **53**, 1358–1364.
207 D. P. Cao and J. Z. Wu, *Carbon*, 2005, **43**, 1364–1370.
208 M. Heuchel, G. M. Davies, E. Buss and N. A. Seaton, *Langmuir*, 1999, **15**, 8695–8705.
209 D. M. Ruthven and S. C. Reyes, *Microporous Mesoporous Mater.*, 2007, **104**, 59–66.
210 S. N. Vyas, S. R. Patwardhan, S. Vijayalakshmi and K. Ganesh, *J. Colloid Interface Sci.*, 1994, **168**, 275–280.
211 M. A. Ahmad, W. M. A. W. Daud and M. K. Aroua, *J. Oil Palm Res.*, 2008, **20**, 453–460.
212 M. A. Ahmad, W. M. A. W. Daud and M. K. Aroua, *Colloids Surf., A*, 2008, **312**, 131–135.
213 W. M. A. W. Daud, M. A. Ahmad and M. K. Aroua, *Sep. Purif. Technol.*, 2007, **57**, 289–293.
214 P. J. M. Carrott, I. P. P. Cansado and M. M. L. Ribeiro Carrott, *Appl. Surf. Sci.*, 2006, **252**, 5948–5952.
215 S. W. Rutherford and D. D. Do, *Langmuir*, 2000, **16**, 7245–7254.
216 S. W. Rutherford and D. D. Do, *Carbon*, 2000, **38**, 1339–1350.
217 S. W. Rutherford and J. E. Coons, *Carbon*, 2003, **41**, 405–411.
218 J. M. V. Nabais, P. J. M. Carrott, M. M. L. R. Carrott, A. M. Padre-Eterno, J. A. Menendez, A. Dominguez and A. L. Ortiz, *Carbon*, 2006, **44**, 1158–1165.

219 A. Jayaraman, A. S. Chiao, J. Padin, R. T. Yang and C. L. Munson, *Sep. Sci. Technol.*, 2002, **37**, 2505–2528.
220 M. C. Campo, F. D. Magalhães and A. Mendes, *J. Membr. Sci.*, 2010, **346**, 15–25.
221 D. S. Lafyatis, J. Tung and H. C. Foley, *Ind. Eng. Chem. Res.*, 1991, **30**, 865–873.
222 R. K. Mariwala and H. C. Foley, *Ind. Eng. Chem. Res.*, 1994, **33**, 607–615.
223 T. X. Nguyen and S. K. Bhatia, *Asia-Pac. J. Chem. Eng.*, 2009, **4**, 557–562.
224 A. A. Fomkin, *Prot. Met. Phys. Chem. Surf.*, 2009, **45**, 121–136.
225 E. Pantatosaki, D. Psomadopoulos, T. Steriotis, A. K. Stubos, A. Papaioannou and G. K. Papadopoulos, *Colloids Surf., A*, 2004, **241**, 127–135.
226 T. A. Steriotis, G. K. Papadopoulos, A. K. Stubos and N. Kanellopoulos, *Stud. Surf. Sci. Catal.*, 2002, **144**, 545–552.
227 S. Samios, G. K. Papadopoulos, T. Steriotis and A. K. Stubos, *Mol. Simul.*, 2001, **27**, 441–456.
228 S. Samios, A. K. Stubos, G. K. Papadopoulos, N. K. Kanellopoulos and F. Rigas, *J. Colloid Interface Sci.*, 2000, **224**, 272–290.
229 A. Vishnyakov, P. I. Ravikovitch and A. V. Neimark, *Langmuir*, 1999, **15**, 8736–8742.
230 S. Samios, A. K. Stubos, N. K. Kanellopoulos, R. F. Cracknell, G. K. Papadopoulos and D. Nicholson, *Langmuir*, 1997, **13**, 2795–2802.
231 M. Cinke, J. Li, C. W. Bauschlicher Jr., A. Ricca and M. Meyyappan, *Chem. Phys. Lett.*, 2003, **376**, 761–766.
232 J. Zhao, A. Buldum, J. Han and J. P. Lu, *Nanotechnology*, 2002, **13**, 195–200.
233 A. Ansón, J. Jagiello, J. B. Parra, M. L. Sanjuán, A. M. Benito, W. K. Maser and M. T. Martínez, *J. Phys. Chem. B*, 2004, **108**, 15820–15826.
234 W. L. Yim, O. Byl, J. T. Yates Jr. and J. K. Johnson, *J. Chem. Phys.*, 2004, **120**, 5377–5386.
235 C. Matranga, L. Chen, M. Smith, E. Bittner, J. K. Johnson and B. Bockrath, *J. Phys. Chem. B*, 2003, **107**, 12930–12941.
236 F. S. Su, C. S. Lu, W. F. Cnen, H. L. Bai and J. F. Hwang, *Sci. Total Environ.*, 2009, **407**, 3017–3023.
237 P. I. Ravikovitch, A. Vishnyakov, R. Russo and A. V. Neimark, *Langmuir*, 2000, **16**, 2311–2320.
238 L. L Huang, L. Z. Zhang, Q. Shao, L. H. Lu, X. H. Lu, S. Y. Jiang and W. F. Shen, *J. Phys. Chem. C*, 2007, **111**, 11912–11920.
239 M. Konstantakou, T. A. Steriotis, G. K. Papadopoulos, M. Kainourgiakis, E. S. Kikkinides and A. K. Stubos, *Appl. Surf. Sci.*, 2007, **253**, 5715–5720.
240 A. I. Skoulidas, D. S. Sholl and J. K. Johnson, *J. Chem. Phys.*, 2006, **124**, 054708.
241 S. B. Sinnott, Z. A. Mao and K. H. Lee, *CMES Comput. Model. Eng. Sci.*, 2002, **3**, 575–587.
242 L. F. Xu, M. Sahimi and T. T. Tsotsis, *Phys. Rev. E: Stat. Phys., Plasmas, Fluids, Relat. Interdiscip. Top.*, 2000, **62**, 6942–6948.
243 L. F. Xu, M. G. Sedigh, T. T. Tsotsis and M. Sahimi, *J. Chem. Phys.*, 2000, **112**, 910–922.
244 E. A. Müller, *J. Phys. Chem. B*, 2008, **112**, 8999–9005.
245 J. C. Su and A. C. Lua, *Sep. Purif. Technol.*, 2009, **69**, 161–167.
246 Y. X. Jia, M. Wang, L. Y. Wu and C. J. Gao, *Sep. Sci. Technol.*, 2007, **42**, 3681–3695.
247 Q. Y. Yang and C. L. Zhong, *Can. J. Chem. Eng.*, 2004, **82**, 580–589.
248 P. A. Gauden and M. Wiśniewski, *Appl. Surf. Sci.*, 2007, **253**, 5726–5731.
249 A. P. Terzyk, S. Furmaniak, P. A. Gauden and P. Kowalczyk, *Adsorpt. Sci. Technol.*, 2009, **27**, 281–296.
250 K. Urita, S. Seki, S. Utsumi, D. Noguchi, H. Kanoh, H. Tanaka, Y. Hattori, Y. Ochiai, N. Aoki, M. Yudasaka, S. Iijima and K. Kaneko, *Nano Lett.*, 2006, **6**, 1325–1328.
251 O. Dewaele and G. F. Froment, *Appl. Catal., A*, 1999, **185**, 203–210.
252 Z. Yong, V. Mata and A. E. Rodrigues, *J. Chem. Eng. Data*, 2000, **45**, 1093–1095.
253 K. Pokrovski, K. T. Jung and A. T. Bell, *Langmuir*, 2001, **17**, 4297–4303.
254 C. Knoefel, V. Hornebecq and P. L. Llewellyn, *Langmuir*, 2008, **24**, 7963–7969.
255 C. Schumacher, J. Gonzalez, M. Perez-Mendoza, P. Wright and N. Seaton, *Ind. Eng. Chem. Res.*, 2006, **45**, 5586–5597.
256 Y. He and N. A. Seaton, *Langmuir*, 2006, **22**, 1150–1155.
257 T. Yoshioka, M. Asaeda and T. Tsuru, *J. Membr. Sci.*, 2007, **293**, 81–93.
258 X. N. Yang, Z. J. Xu and C. J. Zhang, *J. Colloid Interface Sci.*, 2006, **297**, 38–44.
259 H. Takaba, E. Matsuda and S. I. Nakao, *J. Phys. Chem. B*, 2004, **108**, 14142–14147.
260 T. Yoshioka, T. Tsuru and M. Asaeda, *Sep. Purif. Technol.*, 2001, **25**, 441–449.
261 O. Leal, C. Bolivar, C. Ovalles, J. J. Garcia and Y. Espidel, *Inorg. Chim. Acta*, 1995, **240**, 183–189.
262 G. P. Knowles, S. W. Delaney and A. L. Chaffee, *Stud. Surf. Sci. Catal.*, 2005, **156**, 887.
263 G. P. Knowles, J. V. Graham, S. W. Delaney and A. L. Chaffee, *Fuel Process. Technol.*, 2005, **86**, 1435–1448.
264 S. Kim, J. Ida, V. V. Guliants and J. Y. S. Lin, *J. Phys. Chem. B*, 2005, **109**, 6287–6293.
265 R. A. Khatri, S. S. C. Chuang, Y. Soong and M. Gray, *Energy Fuels*, 2006, **20**, 1514–1520.
266 R. Serna-Guerrero, E. Da'na and A. Sayari, *Ind. Eng. Chem. Res.*, 2008, **47**, 9406–9412.
267 A. L. Chaffee, G. P. Knowles, Z. J. Liang, J. Zhany, P. Xiao and P. A. Webley, *Int. J. Greenhouse Gas Control*, 2007, **1**, 11–18.
268 E. Angeletti, C. Canepa, G. Martinetti and P. Venturello, *J. Chem. Soc., Perkin Trans. 1*, 1989, 105–107.
269 S. Che, A. E. Garcia-Bennett, T. Yokoi, K. Sakamoto, H. Kunieda, O. Terasaki and T. Tatsumi, *Nat. Mater.*, 2003, **2**, 801–805.
270 G. Y. Zhao, B. Aziz and N. Hedin, *Appl. Energy*, 2010, **87**, 2907–2913.
271 S. Udayakumar, S. W. Park, D. W. Park and B. S. Choi, *Catal. Commun.*, 2008, **9**, 1563–1570.
272 J. M. Rosenholm, A. Penninkangas and M. Linden, *Chem. Commun.*, 2006, 3909–3911.
273 J. H. Drese, S. Choi, R. P. Lively, W. J. Koros, D. J. Fauth, M. L. Gray and C. W. Jones, *Adv. Funct. Mater.*, 2009, **19**, 3821–3832.
274 X. C. Xu, C. S. Song, B. G. Miller and A. W. Scaroni, *Ind. Eng. Chem. Res.*, 2005, **44**, 8113–8119.
275 X. C. Xu, C. S. Song, B. G. Miller and A. W. Scaroni, *Fuel Process. Technol.*, 2005, **86**, 1457–1472.
276 X. C. Xu, C. S. Song, J. M. Andrésen, B. G. Miller and A. W. Scaroni, *Microporous Mesoporous Mater.*, 2003, **62**, 29–45.
277 X. C. Xu, C. S. Song, J. M. Andresen, B. G. Miller and A. W. Scaroni, *Int. J. Environ. Technol. Manage.*, 2004, **4**, 32–52.
278 T. Montanari and G. Busca, *Vib. Spectrosc.*, 2008, **46**, 45–51.
279 R. W. Stevens, R. V. Siriwardane and J. Logan, *Energy Fuels*, 2008, **22**, 3070–3079.
280 N. Hiyoshi, K. Yogo and T. Yashima, *Microporous Mesoporous Mater.*, 2005, **84**, 357–365.
281 R. A. Khatri, S. S. C. Chuang, Y. Soong and M. Gray, *Ind. Eng. Chem. Res.*, 2005, **44**, 3702–3708.
282 A. C. C. Chang, S. S. C. Chuang, M. Gray and Y. Soong, *Energy Fuels*, 2003, **17**, 468–473.
283 C. W. Hoerr, H. J. Harwood and G. V. Ramarao, *J. Org. Chem.*, 1944, **9**, 201.
284 K. P. Battjes, A. M. Barolo and P. Dreyfuss, *J. Adhes. Sci. Technol.*, 1991, **5**, 785–799.
285 M. Aresta and E. Quaranta, *Tetrahedron*, 1992, **48**, 1515–1530.
286 A. Dibenedetto, M. Aresta, C. Fragale and M. Narracci, *Green Chem.*, 2002, **4**, 439–443.
287 Y. Belmabkhout and A. Sayari, *Adsorption*, 2009, **15**, 318–328.
288 N. Hiyoshi, K. Yogo and T. Yashima, *J. Jpn. Pet. Inst.*, 2005, **48**, 29–36.
289 Z. Bacsik, R. Atluri, A. E. Garcia-Bennett and N. Hedin, *Langmuir*, 2010, **26**, 10013–10024.
290 M. L. Gray, Y. Soong, K. J. Champagne, J. Baltrus, R. W. Stevens, P. Toochinda and S. S. C. Chuang, *Sep. Purif. Technol.*, 2004, **35**, 31–36.
291 C. Y. Lu, H. L. Bai, B. L. Wu, F. S. Su and J. F. Hwang, *Energy Fuels*, 2008, **22**, 3050–3056.
292 E. P. Dillon, C. A. Crouse and A. R. Barron, *ACS Nano*, 2008, **2**, 156–164.
293 A. L. Chaffee, *Fuel Process. Technol.*, 2005, **86**, 1473–1486.
294 L. J. Chen, A. Laaksonen, submitted.
295 Z. Yong, V. Mata and A. E. Rodriguez, *Ind. Eng. Chem. Res.*, 2001, **40**, 204–209.
296 S. P. Reynolds, A. D. Ebner and J. A. Ritter, *Environ. Prog.*, 2006, **25**, 334–342.

297 S. P. Reynolds, A. D. Ebner and J. A. Ritter, *Ind. Eng. Chem. Res.*, 2006, **45**, 4278–4294.
298 S. P. Reynolds, A. Mehrotra, A. D. Ebner and J. A. Ritter, *Adsorption*, 2008, **14**, 399–413.
299 A. D. Ebner, S. P. Reynolds and J. A. Ritter, *Ind. Eng. Chem. Res.*, 2007, **46**, 1737–1744.
300 C. T. Yavuz, B. D. Shinall, A. V. Iretskii, M. G. White, T. Golden, M. Atilhan, P. C. Ford and G. D. Stucky, *Chem. Mater.*, 2009, **21**, 3473–3475.
301 K. B. Lee and S. Sircar, *AIChE J.*, 2008, **54**, 2293–2302.
302 S. F. Wu, T. H. Beum, J. I. Yang and J. N. Kim, *Ind. Eng. Chem. Res.*, 2007, **46**, 7896–7899.
303 A. A. A. Solieman, J. W. Dijkstra, W. G. Haije, P. D. Cobden and R. W. van den Brink, *Int. J. Greenhouse Gas Control*, 2009, **3**, 393–400.
304 A. Duffy, G. M. Walker and S. J. Allen, *Chem. Eng. J.*, 2006, **117**, 239–244.
305 N. Rajabbeigi, B. Elyassi, T. T. Tsotsis and M. Sahimi, *J. Membr. Sci.*, 2009, **335**, 5–12.
306 N. Rajabbeigi, T. T. Tsotsis and M. Sahimi, *J. Membr. Sci.*, 2009, **345**, 323–330.
307 F. Bulnes, A. J. Ramirez-Pastor and V. D. Pereyra, *J. Mol. Catal. A: Chem.*, 2001, **167**, 129–139.
308 C. Santschi and M. J. Rossi, *J. Phys. Chem. A*, 2006, **110**, 6789–6802.
309 C. M. Mömming, S. Frömel, G. Kehr, R. Fröhlich, S. Grimme and G. Erker, *J. Am. Chem. Soc.*, 2009, **131**, 12280–12289.
310 C. M. Mömming, E. Otten, G. Kehr, R. Fröhlich, S. Grimme, D. W. Stephan and G. Erker, *Angew. Chem., Int. Ed.*, 2009, **48**, 6643–6646.